Experimental Investigation and Three-Dimensional Computational Fluid-Dynamics Modeling of the Flash-Converting Furnace Shaft: Part I. Experimental Observation of Copper Converting Reactions in Terms of Converting Rate, Converting Quality, Changes in Particle Size, Morphology, and Mineralogy

MANUEL PEREZ-TELLO, HONG YONG SOHN, KIRSI ST. MARIE, and ARI JOKILAAKSO

An experimental investigation was conducted to elucidate the main features of the processes taking place in the shaft of a continuous flash-converting furnace for solid copper mattes. The experiments were conducted in a large laboratory furnace. The test variables included the matte grade, oxygen content in the process gas, particle size of the feed material, and oxygen-to-matte ratio. The observed variables included the fractional completion of the oxidation reactions, fraction of sulfur remaining in the particles, copper-to-iron atomic ratio, particle-size distribution, morphology, and mineralogy of the reacted particles. The experiments showed substantial differences in the oxidation behavior of high-grade (72 pct Cu) and low-grade (58 pct Cu) matte particles. Low-grade matte particles reacted evenly throughout the furnace, increased in size, and experienced no substantial fragmentation during oxidation. High-grade matte particles tended to be oxidized unevenly and experienced severe fragmentation leading to generation of dust. The order of the effects of the test variables on the observed variables was found to be (1) the oxygen-to-matte ratio, (2) the particle size of the feed material, and (3) the oxygen content in the process gas. Microscopic examination revealed that the oxides of copper and iron were the main oxidation products, with little elemental copper present in the reacted particles. Potential implications of the experimental findings on the operation of an industrial flash-converting furnace are discussed.

I. INTRODUCTION

THE Kennecott–Outokumpu flash-converting process is a new technology to produce blister copper. This process incorporates the principles of the Outokumpu flash-smelting process in the converting step of coppermaking. The flash-converting process is aimed at replacing the converting of molten copper matte in Peirce–Smith converters.

In the flash-converting process (Figure 1), fine copper matte particles and flux particles are fed into a furnace shaft, where a high-strength oxygen-enriched gas stream is injected. In the reaction shaft, the particles are quickly dispersed, heated by the reactor walls and the gas until ignition, partly oxidized, and melted. The molten particles settle in the furnace bottom, where incompletely oxidized sulfides react with metal oxides to produce blister copper, and the blister copper and slag phases are separated.

Some of the key benefits of the flash-converting process include[1–5] continuous operation, little emission of gaseous pollutants, and avoidance of the handling of molten matte. The first industrial-scale application of the flash-converting process was started at the Utah copper smelter in 1995.[2,3] These features make this the cleanest copper converting process currently in operation. Emissions are highly controlled, with sulfur capture in excess of 99.9 pct, equivalent to 3 kg of SO_2 per tonne of copper, the lowest emission in the world.[5]

Although the flash-converting process has been under development since the early 1980s, experimental data on its performance have been rather scarce until recently. Asteljoki *et al.*[1] and Asteljoki and Kytö[4] reported on experimental data from a flash-converting pilot-scale facility. They analyzed the copper losses in the slag phase and the distribution of minor elements between the blister copper and slag in the settler. Whereas the residence time of the particles in the shaft is of the order of seconds, the residence time of the melt and slag in the settler is of the order of hours. Therefore, the information concerning the behavior of gas and particles in the reaction shaft was not available from these tests.

Suominen *et al.*[6,7] reported on oxidation tests of industrial copper matte particles in a laminar-flow reactor. Test variables included the particle size, matte grade, and oxygen concentration in the process gas. Variables measured in the experiments included the percentage of the initial sulfur left in the particles and the morphology and mineralogy of the

MANUEL PEREZ-TELLO, formerly Graduate Student, Department of Chemical and Fuels Engineering, University of Utah, is Associate Professor, Department of Chemical Engineering and Metallurgy, University of Sonora, Sonora, Mexico 83000. HONG YONG SOHN, Professor, is with the Department of Metallurgical Engineering, University of Utah, Salt Lake City, UT 84112. KIRSI ST. MARIE, formerly Research Associate, Department of Metallurgical Engineering, University of Utah, Engineer, is with Reaction Engineering International, Salt Lake City, UT 84101. ARI JOKILAAKSO, Docent, is with the Department of Materials Science and Rock Engineering, Helsinki University of Technology, FIN-02150 Espoo, Finland.

Manuscript submitted May 26, 2000.

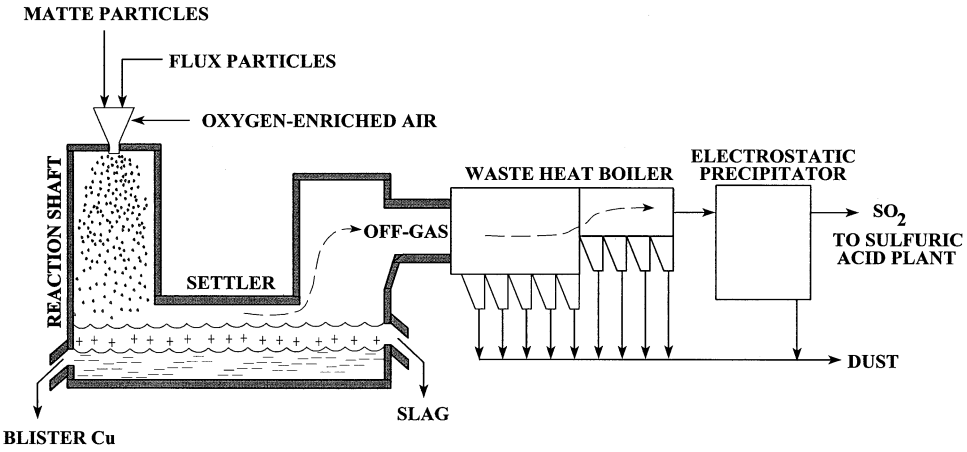

Fig. 1—Flash converting process of solid copper mattes.

reacted particles. The experimental results showed that particle reactivity increased with increasing gas temperature and oxygen concentration and decreased with increasing matte grade and particle size. Overall, matte particles were less reactive than copper-concentrate particles. However, under the highly oxidizing conditions attained with a high oxygen concentration (75 vol pct) and high gas temperature (1100 °C), matte particles reacted extensively, regardless of their particle size and matte grade. The oxidized particles produced a significant amount of dust as a result of fragmentation. The results by Suominen *et al.*[6,7] showed that the reaction path during particle oxidation is strongly dependent on the initial matte grade, particle size, and local conditions surrounding the particles. The authors adapted the reaction path originally proposed by Kim and Themelis[8] for the oxidation of sulfide particles to explain the physicochemical transformations observed in their experiments.

In this laboratory, differential scanning calorimetry and thermogravimetric analysis were used to study the oxidation behavior of copper matte particles.[9] Test variables were the oxygen concentration in the reacting gas, matte grade, and particle size. Measured variables were the particle temperature, total heat released by the exothermic processes, total heat absorbed by the endothermic processes, and the weight of the particles as they underwent oxidation.

The chemical changes experienced by the particles were explained in terms of seven chemical reactions. The oxidation of the iron sulfide was assumed to occur first as $FeS \rightarrow FeO \rightarrow Fe_3O_4 \rightarrow Fe_2O_3$. Then the copper sulfide was assumed to react, according to $Cu_2S \rightarrow Cu_2O \rightarrow (CuO \cdot CuSO_4) \rightarrow CuO$. The mechanism assumed that successive layers of Cu_2O, $CuO \cdot CuSO_4$, and CuO were formed within the particles.

The results obtained in this laboratory[9] qualitatively agreed with the observations by Suominen *et al.*[6,7] in a laminar-flow reactor. Quantitatively, the temperatures of the incipient reaction measured in this laboratory[14] (467 °C to 618 °C) were considerably lower than the ignition temperatures reported by Suominen *et al.*,[7,8] which were higher than 800 °C. The temperature of the incipient reaction does not represent an ignition process, in which the reactions become self-sustained. Rather, it represents the temperature at which the rate of the reaction starts a rapid increase with temperature, a kinetic property of the material. On the other hand, the ignition temperature depends on heat- and mass-transfer effects between the particle and its surroundings.

The combustion of "MK" concentrate particles has been studied by researchers at the University of British Columbia.[10–14] The composition of the MK concentrate particles closely resembles that of high-grade copper matte particles. Morgan *et al.*[10] summarized the relevant results of the investigations. Both laboratory-scale[11,12] and pilot-scale[10] experiments were conducted. Laboratory experiments involved pyrometry techniques to measure particle temperatures at the exit of a laminar-flow reactor. Pilot tests were used to validate a combustion flame mathematical model[13] and to test the effect of different burner configurations on the amount of dust produced in the reaction shaft. Shook *et al.*[14] developed a kinetic model for the oxidation of single MK concentrate particles. They also suggested a dust generation mechanism based on two possible phenomena: (1) copper volatilization followed by gas-phase oxidation and condensation, and (2) the boiling of copper in the particle followed by particle fragmentation.

Suominen *et al.*[6,7] and Shook *et al.*[14] pointed out the relevance of the dust generation mechanisms during the oxidation of copper matte particles. In both flash smelting and flash converting, dust is generated by small or fragmented large feed particles and by condensation of volatile components. Although, in practice, dust is usually recycled to the furnace, its generation is undesirable because it accumulates in the connection between the uptake shaft and the waste-heat boiler inlet and in the off-gas ducts (Figure 1). When doing so, it can throttle the off-gas lines. If the composition of the dust is not controlled, it also builds up on the boiler-tube surfaces, decreasing steam production and boiler capacity can cause corrosion problems and plug the pneumatic transport system. Thus, control of the dust level is an important factor in the optimization of industrial flash-smelting/flash-converting furnaces.

Overall, the experimental studies on flash converting reported in the literature suggest that the reaction mechanisms are complex and strongly dependent on the local conditions surrounding the particles. The exact stoichiometry of the reactions occurring in the shaft is unknown. In addition to chemical changes experienced by the particles,

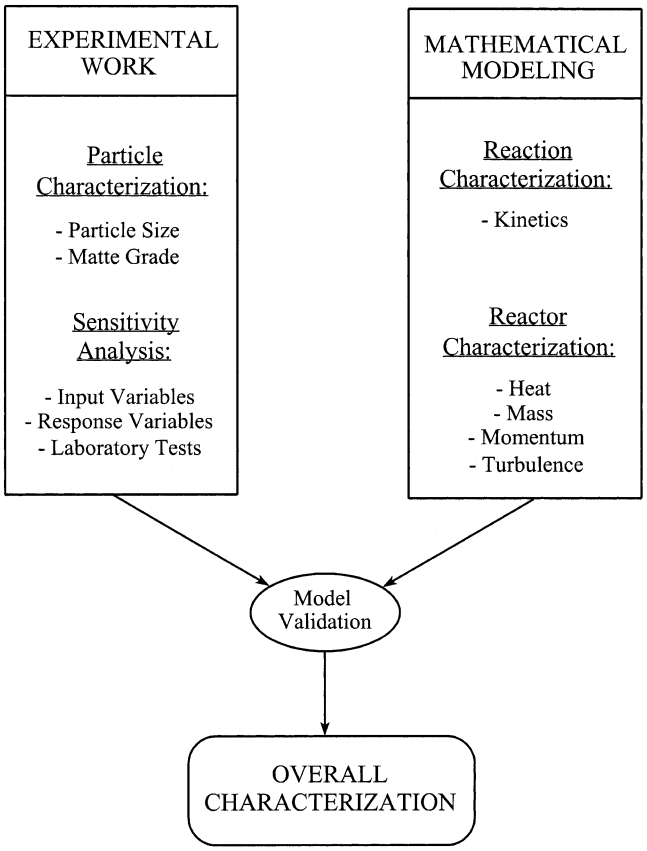

Fig. 2—Overall strategy of this investigation.

physical transformations such as melting, gas buildup, explosion, and, possibly, boiling[14] are to be expected. The complexity of the reaction path complicates the understanding of it on a fundamental basis.

At the University of Utah, an extensive research program on the flash-converting process has been underway since 1994. The goal of this investigation was to characterize from a fundamental standpoint the major subprocesses occurring in the flash-converting furnace shaft. In order to achieve this goal, a combined experimental and modeling approach has been followed. The overall strategy is schematically presented in Figure 2.

The present series of three articles summarizes the relevant results of the strategy outlined in Figure 2. Part I deals with the experimental work conducted in a large laboratory furnace; Part II describes the development of a comprehensive three-dimensional computational fluid-dynamics model of the flash-converting furnace shaft and its verification with the experimental data; and Part III reports the simulation of an industrial flash-converting operation.

A summary of the results of this investigation is presented in this series; a more detailed discussion is presented elsewhere.[15] Various early descriptions of experimental[16–19] and computer-modeling[20] aspects of this investigation were reported by the present authors.

II. EXPERIMENTAL WORK

The goal of the experimental work was twofold: (1) to determine the effects of furnace conditions on the flash-converting operation under controlled conditions, and (2) to provide experimental data to validate the computer model described in Part II of this series.

A. *Experimental Facility*

The experimental setup used in this study is shown schematically in Figure 3. It consisted of five units: a solids and gas feeding unit, a reaction shaft, a product receptacle, a sampling probe, and an off-gas unit. The experimental setup was similar to that used in the past at the University of Utah to carry out flash-smelting studies.[21]

The reaction shaft was a large laboratory furnace consisting of a vertical, one-piece cast alumina ceramic cylinder. Its i.d. was 0.24 m, its height was 1.4 m, and its wall thickness was 0.025 m. The reaction shaft was surrounded by six heating elements located 0.02 m away from the outer wall. Eight Pt-Pt 10 pct Rh thermocouples were placed along the outer wall of the reaction chamber; the thermocouples were interfaced to a computer for continuous recording of wall temperatures. The maximum wall temperature attained in the experimental setup was 1100 °C ± 30 °C.

Granulated and ground copper matte particles were stored in a 10 dm^3 hopper and fed into the furnace with a single-screw feeder. The process gas was supplied by two rotameters handling pure oxygen and air, respectively, at room conditions (86.1 kPa in Salt Lake City and 298 K). The feed rate of the particles was fixed at 3 kg/h, and the volumetric gas flow rate was adjusted to satisfy the conditions to be tested.

Matte particles and gas entered the furnace through a water-cooled Outokumpu-type pilot-scale burner (Figure 4). The burner had a 2 cm opening at the center, which was used as the primary stream for the particles. The oxidizing gas, a mixture of air and oxygen, was divided into six jets (secondary stream), entering the furnace through six 2-mm-diameter nozzles at the burner tip. The gas jets from the burner were aimed to converge at a centerline position 25 cm below the burner tip.

The copper matte particles were oxidized while flowing downward with the gas and were collected in the receptacle (Figure 5). The lower part of the receptacle was detachable, fixed to the shaft body by bolts, and externally water cooled by a copper coil. The goal of the receptacle was to quench the particles falling from the shaft, thus interrupting the oxidation reactions, and collect them for further analysis. The steel cooling section of the receptacle had a side-stream opening for the exhaust gas. The particles settled in the receptacle, while a small fraction (less than 1 pct) followed the exhaust gas.

On the bottom of the receptacle there was a centered 0.05-m-wide opening for the sampling probe. The probe consisted of two stainless steel tubes placed concentrically (Figure 6); it was internally water cooled through the annulus and was connected to a cylindrical sampler. A low suction was applied through the sampler and probe to provide an isokinetic sampling.

The off-gas unit consisted of a 25-cm-diameter glass scrubber, packed with $^1/_2$-inch ceramic Berl saddles. A 6 pct NaOH aqueous solution was used as the absorbent.

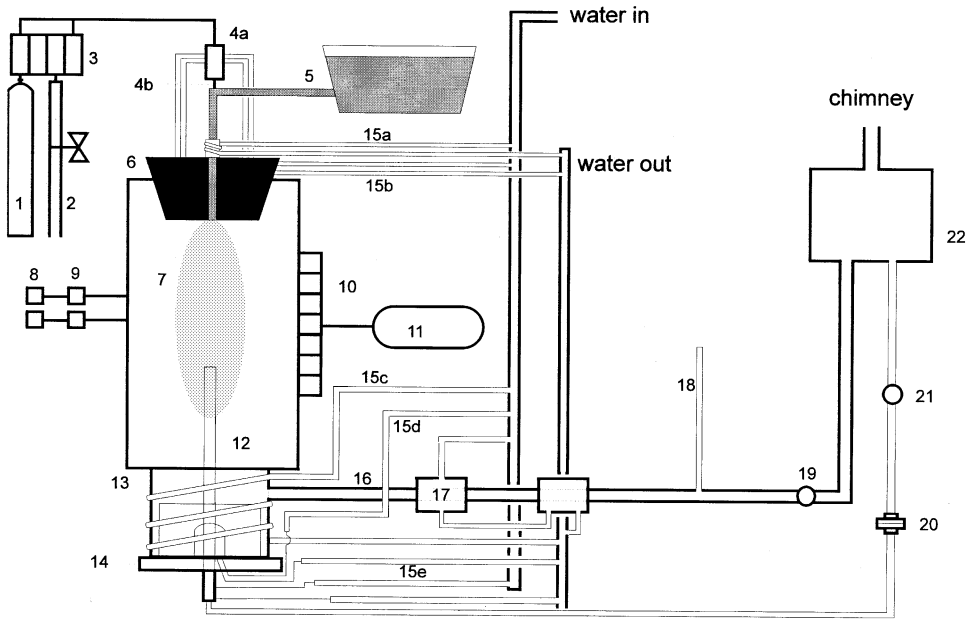

Fig. 3—Figure 3. Experimental setup: (1) oxygen cylinder, (2) compressed air, (3) gas flow meters, (4a) gas distributor, (4b) process gas, (5) screw f eeder, (6) burner, (7) reaction shaft, (8) power switches, (9) temperature controllers, (10) thermocouples, (11) computer, (12) sampling probe, (13) gas and particle cooling section, (14) particle receptacle, (15a) to (15e) cooling water, (16) exhaust gas line, (17) heat exchanger, (18) manometer, (19) gas valve, (20) particle probe sampler, (21) vacuum pump, and (22) scrubber.

B. *Basis of the Experiments and Experimental Program*

The flash-converting process (Figure 1) is aimed at performing the following overall reactions;

$$Cu_2S + O_2 \rightarrow 2Cu + SO_2 \quad [1]$$

$$3FeS + 5O_2 \rightarrow Fe_3O_4 + 3SO_2 \quad [2]$$

i.e., the production of blister copper and the elimination of iron as magnetite dissolved in calcium ferrite slag.

It should be noted that reactions [1] and [2] are not the reactions taking place in the reaction shaft, but they represent the overall converting reactions, including the reactions in the shaft and in the molten bath. Reactions [1] and [2] indicate that the goal of a converting operation is the oxidation of all the sulfur in the matte to SO_2 and of all the iron in the matte to Fe_3O_4.

In the experiments, the feed rate of the particles to the reaction shaft was kept constant. Based on the iron and sulfur content of the particles, the amount of oxygen necessary to carry out reactions [1] and [2] to completion was computed. The actual oxygen supplied with the particles was either equal to or higher than the stoichiometric amount by a fixed ratio. The relative amount of oxygen supplied with the particles is called, in this study, the oxygen-to-matte ratio, or oxygen availability.

It is recognized that the flash-converting process is a complex process in which multiple phenomena occur simultaneously at a microscopic scale. Macroscopically, however, system responses such as sulfur removal, oxygen consumption, and degree of fragmentation seem to be controlled by a limited number of operating variables. In this study, the following operating variables were selected for study: particle size of the feed material, matte grade, oxygen content in the process gas, and amount of oxygen supplied with the particles. The test variables and their range of variations are summarized in Table I.

Particles with two different matte grades were used. A high-grade matte containing 72 pct Cu by weight was from Outokumpu's Harjavalta smelter, produced from a Kennecott concentrate. This matte closely represents the matte processed in the commercial unit.[2] A low-grade matte provided by Outokumpu Oy was also studied. This matte was synthesized by remelting and grinding a 70 pct Cu flash-smelting matte with pyrite (FeS_2) to result in a matte containing 58 pct Cu by weight. Both mattes were granulated, ground, and sieved into the size fractions shown in Table I. The chemical analyses in both mattes did not vary substantially with the particle-size fraction. The average chemical composition of the matte fractions is shown in Table I.

Table II summarizes the variables observed in the reacted particles. They are divided into two groups: directly observed and indirectly observed variables. Directly observed variables were measured directly from the reacted particles. Indirectly observed variables were computed based upon the values of the directly observed variables and by making certain assumptions regarding the nature of the reacting particles.

Whereas most of the observed variables in Table II are self explanatory, the variables of the fractional conversion and converting-quality index must be explained. In this study, fractional conversion was defined as

$$\text{Fractional Conversion} = 1 - (OR)_{sample}/(OR)_{feed} \quad [3]$$

where $(OR)_{sample}$ and $(OR)_{feed}$ represent the amount of oxygen required to oxidize all sulfur and iron in the sample and the feed particles, respectively, to sulfur dioxide and magnetite. These quantities were computed from the amount of oxygen required to oxidize all sulfur and iron in any particle to sulfur dioxide and magnetite minus the amount of oxygen in any form already in the particle, if any.

Fractional conversion indicates the degree of oxidation of the matte particles. When its value is unity, either all

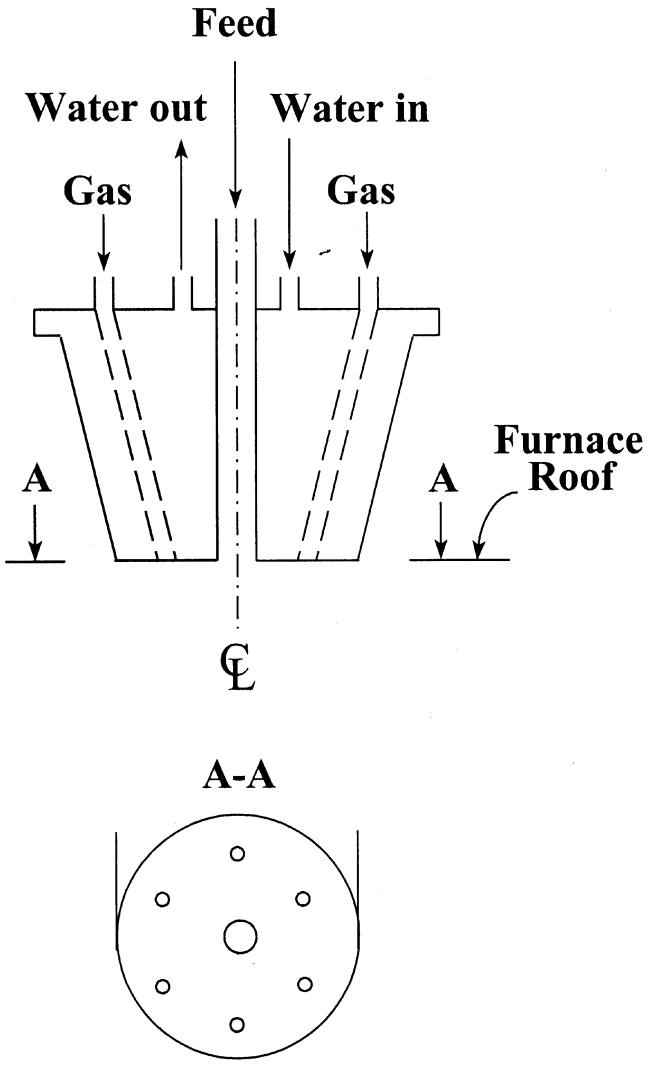

Fig. 4—Schematic diagram of the Outokumpu-type burner used in this study.

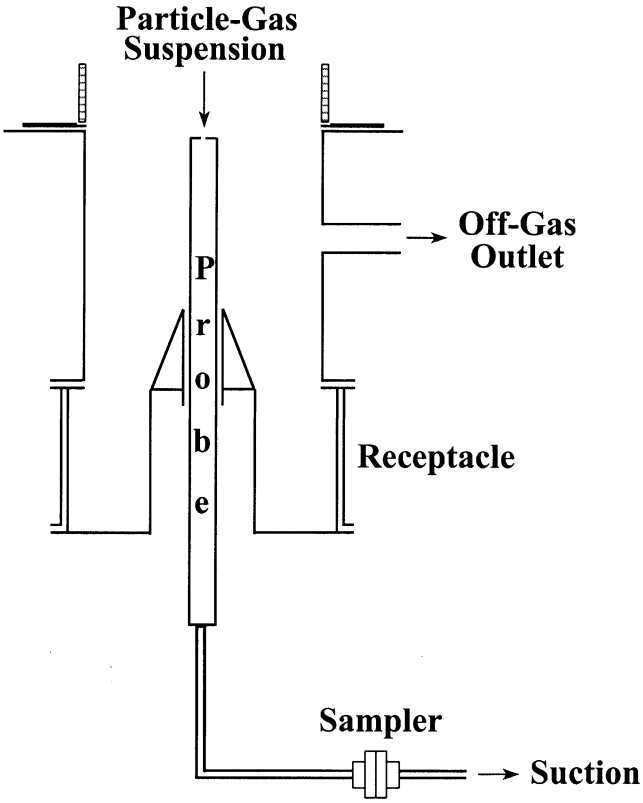

Fig. 5—Schematic diagram of the sampling assembly: receptacle, probe, and sampler.

iron and sulfur have been oxidized to magnetite and sulfur dioxide, or, if the reacted sample contains sulfur, it also contains an excess of oxygen just enough to form sulfur dioxide when it reaches the molten bath. Fractional conversion may take on values higher than unity if the sample is overoxidized.

It is noted that the oxygen-to-matte ratios in Table I were based on the assumption that the matte particles were made up of copper, iron, and sulfur only. To take into account the oxygen initially present in the particles, an estimated maximum conversion was determined as follows:

$$\text{Estimated Maximum Conversion} = \frac{\text{Amount of Oxygen Fed into the Furnace}}{\text{Excess Amount of Oxygen Required for Reactions [1] and [2]}} \quad [4]$$

The denominator in Eq. [4] takes into account the oxygen initially present in the matte particles. Since the fractional conversion is based on the production of elemental copper when converting is complete, both the fractional conversion and the estimated maximum conversion can take on values higher than unity.

Based on Eq. [4] and the data reported in Table I, the expected maximum fractional conversion in the experiments with the 72 pct matte was approximately 1.3 and 1.7 when the oxygen-to-matte ratio was set to 0.25 and 0.33 kg O_2/kg matte, respectively. Similarly, the expected maximum fractional conversion in the experiments with the 58 pct matte was about 1.08 to 1.15.

If the actual fractional conversion attained by the particles is divided by the expected maximum fractional conversion, an estimation of the oxygen consumption in the furnace can be obtained:

$$\text{Oxygen Consumption} = \frac{\text{Fractional Conversion}}{\text{Maximum Fractional Conversion}} \quad [5]$$

The values of the fractional conversion and sulfur remaining in the particles can be combined to compute the converting-quality index, which was defined as

$$\text{Converting-Quality Index} = 1 - \frac{\text{Fraction of Sulfur Remaining in Particle}}{\text{Fractional Conversion}} \quad [6]$$

The converting-quality index represents the fraction of oxygen consumed by the particles that was used to produce sulfur dioxide and magnetite. Thus, it indicates the quality of the converting operation. The best converting quality is achieved when the converting-quality index is equal to unity. Lower values indicate that not all the oxygen consumed by the particles was used to produce sulfur dioxide and magnetite.

The particle-size distribution of the reacted particles was

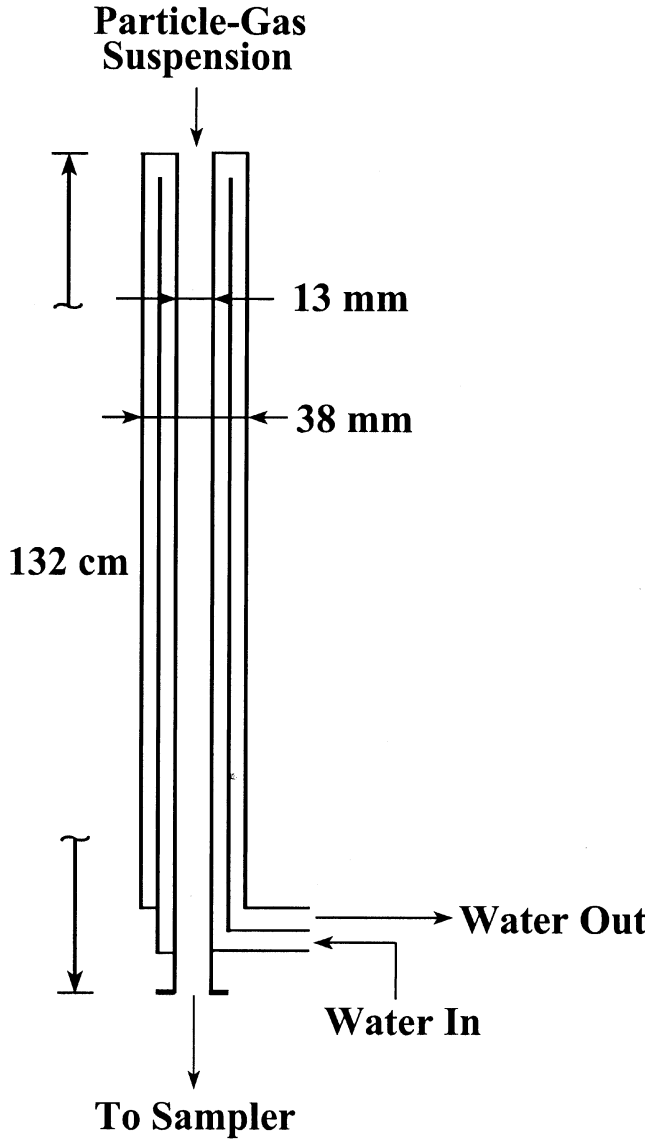

Fig. 6—Schematic diagram of the sampling probe.

Table I. Summary of Test Variables

Test Variable	High-Grade Matte	Low-Grade Matte
Particle composition, wt pct		
Cu	72	58
Fe	4.4	14
S	20.1	25
O	3.5	3
Particle size of the feed, μm	<37	<40
	37 to 74	40 to 74
	74 to 105	75 to 100
	105 to 149	100 to 149
Oxygen content in process gas, vol pct	70 to 100	50 to 100
Oxygen-to-matte ratio, kg oxygen/kg matte	0.25,* 0.33	0.3*

*Stoichiometric amount for Reactions [1] and [2] assuming the particles were made up of copper, iron, and sulfur only.

Table II. Variables Observed in the Reacted Particles

Directly Observed Variables	Indirectly Observed Variables
Chemical analysis:	fractional conversion
wt pct Cu	
wt pct Fe	
wt pct S	sulfur remaining
Particle size distribution by volume	mean size
Dust generation	
Morphology	converting quality index
Mineralogy	copper-to-iron atomic ratio

also measured in the experiments. From these measurements, the change in the mean size of the particle population was computed as follows:

$$\Delta(\text{Mean Size}) = (\text{Mean Size})_{\text{sample}} - (\text{Mean Size})_{\text{feed}} \quad [7]$$

where the mean-size values in the right-hand side of Eq. [7] were calculated from the particle-size distributions by volume of sample and feed, respectively.

Positive values of the left-hand side of Eq. [7] indicated an increase in the mean particle size upon oxidation; negative values indicated a decrease in the mean particle size upon oxidation. The results from Eq. [7] are relevant, as they also signal other phenomena occurring in the reacting particles, such as particle fragmentation or particle expansion.

The particle-size distributions of the feed and reacted particles were also used to determine the amount of dust generated during particle oxidation. In this study, particles smaller than 20 μm were considered dust. The generation of dust was computed from the following expression:

$$\Delta(\text{Volume Fraction of Dust}) = (\text{Volume Fraction of Dust})_{\text{sample}} - (\text{Volume Fraction of Dust})_{\text{feed}} \quad [8]$$

C. *Procedure*

In a typical run, the walls of the reaction chamber were first preheated to the specified temperature (1100 °C ± 30 °C) as a small flow of air passed through the reactor. When the temperature profile displayed on the computer console remained steady at the target temperature, the experiment was started. The sampling probe was placed in its lowest position inside the reaction shaft, the vacuum pump and gas cleaning system were turned on, and the particles and gas were fed to the reactor at the specified rate of the run. The feed rate of the particles was controlled by a screw feeder at the top of the furnace. The gas flow rate was controlled by two rotameters for air and oxygen, so that the total flow and gas composition satisfied the oxygen content and oxygen-to-matte ratio to be tested in the run. The screw feeder and rotameters were calibrated moments before a run was started to minimize experimental uncertainties.

During the experimental run, two to three samples of the reacting particles were collected with the probe along the reactor centerline. The sampling locations corresponded to

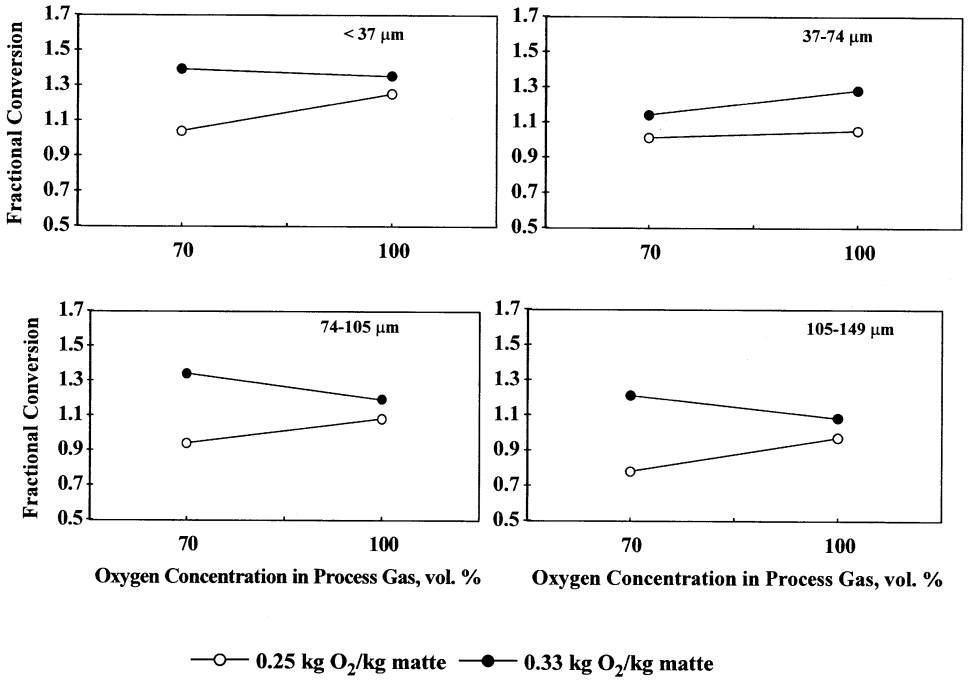

Fig. 7—Fractional conversion of the receptacle samples, 72 pct matte particles.

0.66, 0.86, and 1.72 m below the burner tip. Wall temperatures were continuously monitored through the computer interface. No substantial changes in the temperature profile were detected during the experiments. The manometric pressure in the furnace was typically 0.25 to 0.74 kPa below the atmospheric pressure (86.1 kPa in Salt Lake City) and was simultaneously monitored by a hydrostatic gage connected to the off-gas line and by a manometer located 15 cm above the receptacle. Continuous pressure fluctuations typically indicated blocking of the primary stream with agglomerated, sintered particles. When this occurred, the experiment was shut down, the burner was cleaned, the particles collected in the receptacle were discarded, and the entire run was repeated. At the end of each run, the particles collected through the probe and those deposited in the receptacle were stored and labeled for further analysis.

D. *Analytical Techniques*

The sulfur, copper, and iron in the particles were analyzed. The sulfur was analyzed gravimetrically by burning the sample in air and subsequently determining the amount of sulfur dioxide evolved. The copper and iron analyses were carried out by the standard atomic absorption spectroscopy technique, while oxygen in the feed fractions, whose presence was determined semiquantitatively by hydrogen reduction, was assumed to be the balance. A JEOL* JXA 840A scanning electron microscope (SEM) was used to study the particle fragmentation and morphology of the reacted particles. Changes in composition and internal structure were examined from polished sections by scanning electron microscopy using a Tracor Voyager II energy-dispersive spectrometer and back-scattered electron analysis together with optical microscopy. Particle-size changes were examined by measuring the particle-size distribution by volume for all receptacle samples and feed fractions using a Fritsch particle sizer (Analysette 22).

*JEOL is trademark of Japan Electron Optics Ltd., Tokyo.

III. RESULTS

This section presents a summary of the experimental results obtained and is divided into three parts: parts A and B are devoted to the receptacle samples, and part C discusses the probe samples. A detailed discussion of all the experimental results obtained in this study can be found in Reference 15.

The receptacle samples included all the particles that passed through the reaction shaft and reached the bottom (Figure 3); thus, their properties can be considered to represent the overall process responses to the variables being tested. On the other hand, probe samples represent the local conditions prevailing in the reaction chamber.

A. *High-Grade (72 pct) Matte Feed*

1. *Fractional conversion*

Figure 7 shows the results for the fractional conversion with the high-grade (72 pct) matte. It is noted that an increasing oxygen-to-matte ratio produced an increase in the fractional conversion under all experimental conditions. This trend was expected, since the oxygen-to-matte ratio determines the amount of oxygen available to the particles to react. The effect of the particle size can also be observed by comparing the range of fractional conversion values obtained for different particle-size fractions. As expected, small particles reacted more extensively than large particles. In addition to their larger specific surface area, large particles were heated more slowly by the reactor wall and gas than

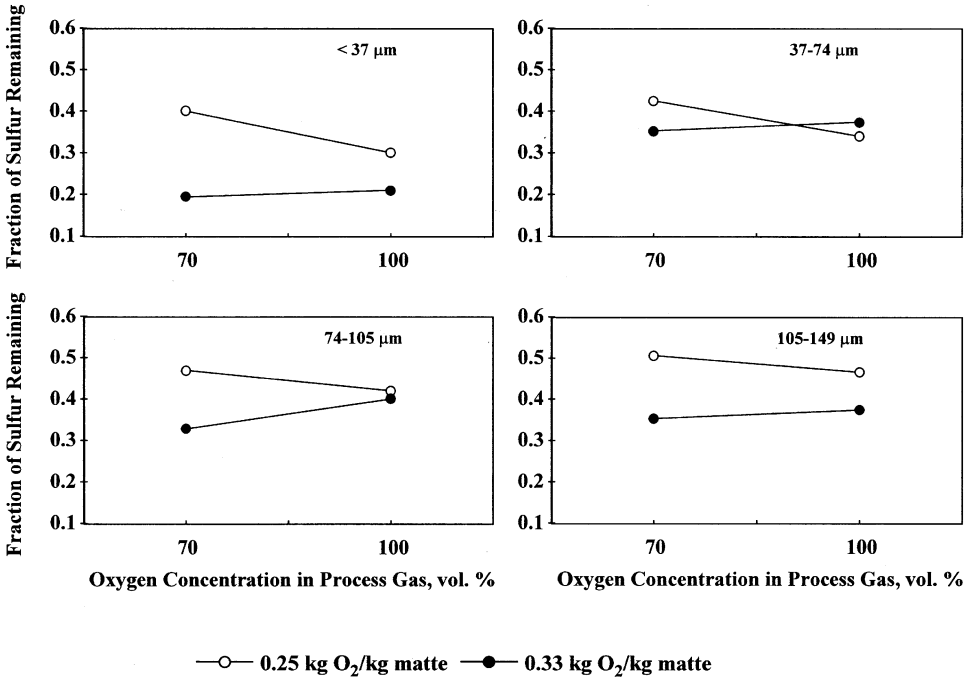

Fig. 8—Sulfur remaining in the receptacle samples, 72 pct matte particles.

were small particles. Thus, the onset of the reaction of large particles occurred farther away from the burner tip.

The effect of oxygen concentration in Figure 7 is indicated by the slope of the lines obtained at a constant oxygen-to-matte ratio. The fractional conversion did not change substantially when the oxygen concentration was varied between 70 pct and pure oxygen. This result was unexpected, because reaction kinetics are thought to be strongly dependent on oxygen partial pressure. Since oxygen was not completely consumed in the experiments, a higher oxygen concentration would be expected to produce a higher degree of particle oxidation. A possible explanation for this behavior is the change in the properties of the oxide layer which surrounds the unreacted core of sulfides during oxidation. With pure oxygen, the oxidation reactions were initially faster than with 70 pct oxygen; thus, the heating rate of the particles was high. A high heating rate may have partially melted the oxide layer, producing the blockage of its pores and, thus, preventing the oxygen molecules from diffusing into the particle. When the pores got blocked, the oxidation rate decreased thereafter.

On the other hand, the effect of hydrodynamics may have also masked the effect of oxygen concentration. In the experiments, the solid feed rate was kept constant, and the gas flow rate was adjusted to satisfy the conditions to be tested. As a result, the hydrodynamic conditions in the furnace were not the same in all the experiments. With a 70 pct oxygen content in the process gas, the volumetric flow rate was 1.4 times larger than with pure oxygen. A larger flow rate produced higher turbulence in the shaft and, thus, a better mixing of the particle-gas suspension than with pure oxygen. It is also noted that the fractional conversion reached values higher than unity in most of the runs; *i.e.*, overoxidation of the matte particles took place, and copper oxides were produced in the particles.

The estimated oxygen consumption computed from Eq. [5] varied between 63 and 91 pct.

2. *Sulfur removal*

The removal of sulfur followed trends similar to those of the fractional conversion and is shown in Figure 8. An increase in oxygen availability increased the amount of sulfur removed from the particles. As expected, small particles were more reactive than large particles. The removal of sulfur from the finest particles (<37 μm in size) varied between 60 and 80 pct, whereas it was 50 to 65 pct for the largest particles (105 to 149 μm in size). Overall, the removal of sulfur was most strongly affected by the oxygen-to-matte ratio, followed by the particle size and oxygen concentration. The trends observed can also be explained by the same hypotheses presented in the discussion of Figure 7.

3. *Converting-quality index*

The converting quality achieved by the 72 pct matte particles is shown schematically in Figure 9. Values varied between 0.4 and 0.7. Since the converting-quality index did not achieve the value of unity in any experiment, not all the oxygen consumed by the particles was used to produce sulfur dioxide and magnetite. This agreed with the fractional-conversion values higher than unity, shown in Figure 7, which indicated that copper oxides were formed within the particles. The effects of the oxygen concentration and oxygen-to-matte ratio did not appear to be significant.

4. *Copper-to-iron atomic ratio*

The copper-to-iron atomic ratio in the receptacle samples did not differ substantially from that of the feed particles. Thus, copper species that possibly volatilized in the reaction flame were precipitated in the receptacle. Overall, copper volatilization in the experiments of the 72 pct matte was negligible.

5. *Mean size*

Particles of the 72 pct matte experienced substantial changes in size upon oxidation. Figure 10 shows the change in the mean size between the receptacle and feed particles

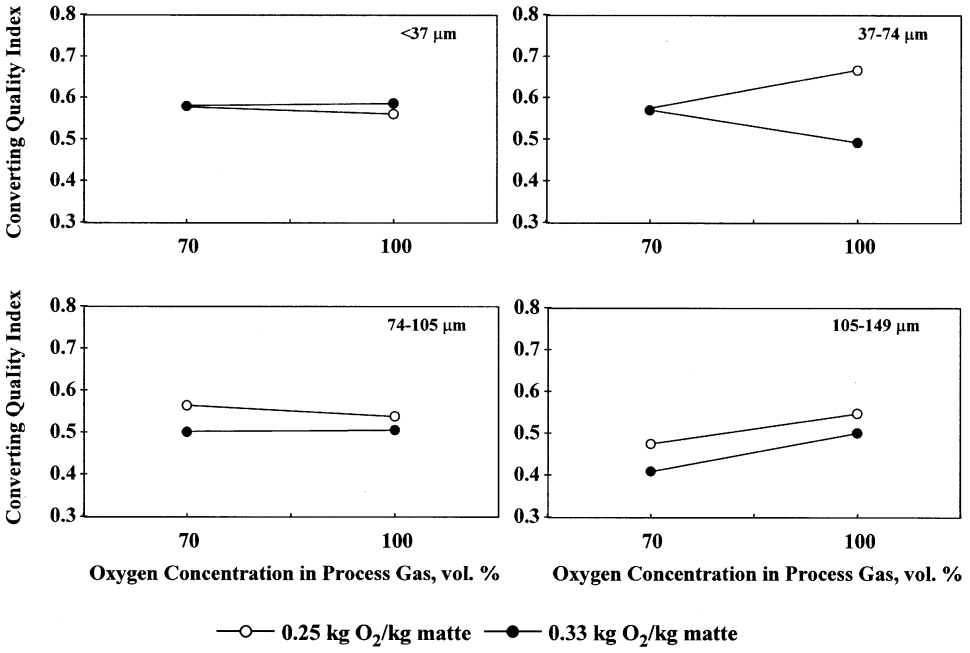

Fig. 9—Converting quality index of the receptacle samples, 72 pct matte particles.

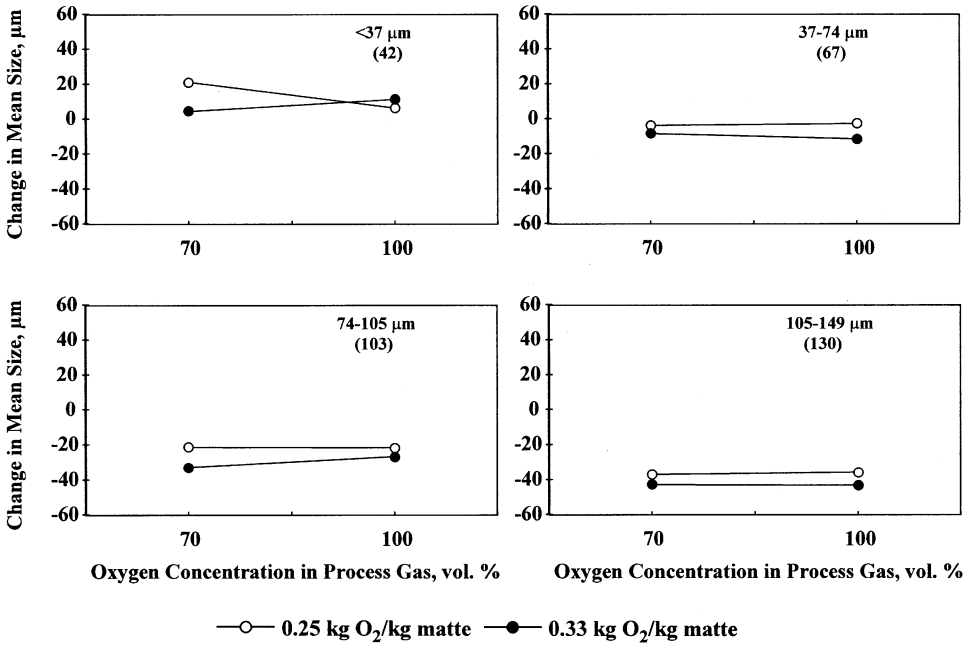

Fig. 10—Change in mean size between receptacle and feed particles, 72 pct matte; values in parentheses indicate the mean size of the feed, in μm.

computed from Eq. [7]. The initial particle size affected the size changes most significantly, whereas the oxygen concentration and oxygen availability did not play a major role. The largest increase in the mean size of the population (20 μm) was achieved by the <37 μm fraction; this change represented more than a 50 pct increase with respect to the size of the feed material. The largest decrease in the mean size of the population (40 μm) was achieved by the 105 to 149 μm fraction, which represented a 35 pct decrease of its initial mean size. On the average, the larger the particles fed to the reactor, the larger the possibility of generating finer particles in the products. Microscopic examination of the particles further suggested that this was caused by extensive fragmentation of the large particles upon oxidation. In contrast, small particles tended to expand upon oxidation.

6. *Dust generation*

As a result of particle fragmentation, all fractions of the 72 pct matte produced dust with varying degrees of severity. This is shown in Figure 11. The generation of dust is indicated by the positive change in dust content in the majority of the experimental conditions. In only one case, the amount of dust particles decreased from that in the feed; this corresponded to the <37 μm fraction reacting under the mildest

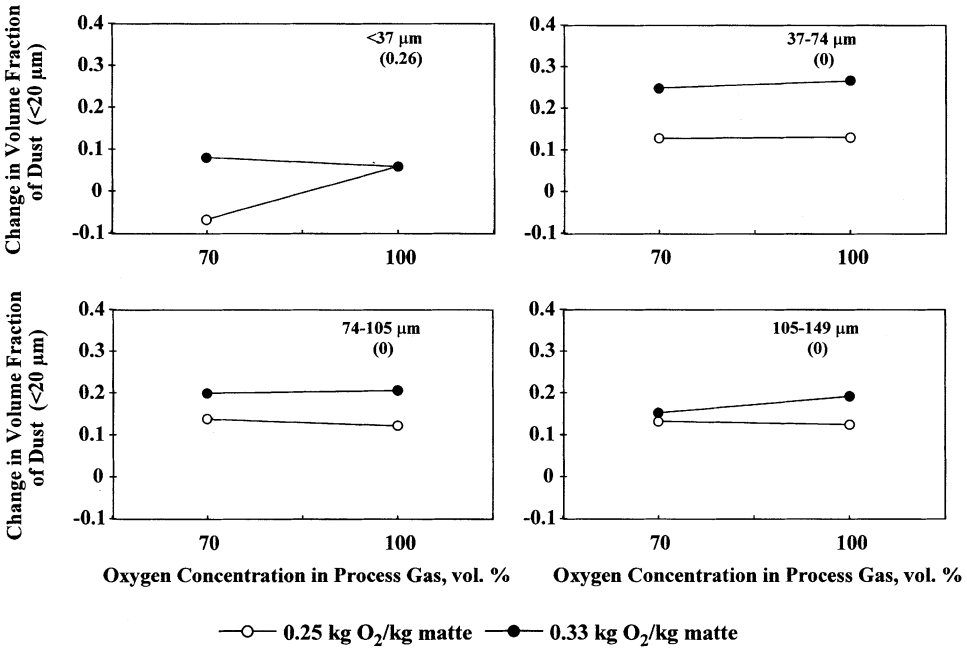

Fig. 11—Change in dust content between receptacle and feed particles, 72 pct matte; values in parentheses indicate the volume fraction of dust partic les (<20 μm) in the feed.

Table III. Summary of Dust Generation Data from the Experiments with the 72 Pct Matte

Run Number	Particle Size Fraction (μm)	Oxygen Content (Vol Pct)	Oxygen-to-Matte Ratio (kg O_2/kg Matte)	Dust Generated* (Pct of the Feed)
1	<37	70	0.25	− 7
2	<37	70	0.33	8
3	<37	100	0.25	6
4	<37	100	0.33	6
5	37 to 74	70	0.25	13
6	37 to 74	70	0.33	25
7	37 to 74	100	0.25	13
8	37 to 74	100	0.33	26
9	74 to 105	70	0.25	14
10	74 to 105	70	0.33	20
11	74 to 105	100	0.25	12
12	74 to 105	100	0.33	20
13	105 to 149	70	0.25	13
14	105 to 149	70	0.33	15
15	105 to 149	100	0.25	12
16	105 to 149	100	0.33	19

*Decrease in dust content if value is negative.

oxidizing conditions (0.25 kg O_2/kg matte and 70 pct O_2). In general, the generation of dust increased with an increasing oxygen-to-matte ratio. This effect was more significant for the fine particles (37 to 74 μm fraction) than for the large particles (105 to 149 μm fraction). Both trends suggest that the generation of dust particles is linked to the rate of the oxidation reactions. The high reactivity of the small particles causes them to respond faster to a change in oxygen availability than the large particles. In general, the oxygen concentration did not affect the generation of dust when it varied between 70 and 100 pct.

On the other hand, the initial particle size of the feed affected the generation of dust to some extent, but this effect does not seem to be as significant as that of the oxygen-to-matte ratio. The generation of dust varied between 6 and 26 pct of the initial feed for all size fractions, as shown in Table III. This estimate does not consider the amount of particles that stuck to the walls and those carried away in the off-gas line. The amount of particles deposited on the walls varied between 0 and 10 pct of the feed and was more significant for the <37 μm fraction. The dust carried away with the gas was less than 0.3 pct of the feed in all the experiments and is not considered to be a significant source of error. Thus, the range of 6 to 26 pct of the feed roughly represents the actual dust generated in the experiments. This is a significant finding, because dust generation is to be avoided during the operation of the industrial flash-converting furnace.

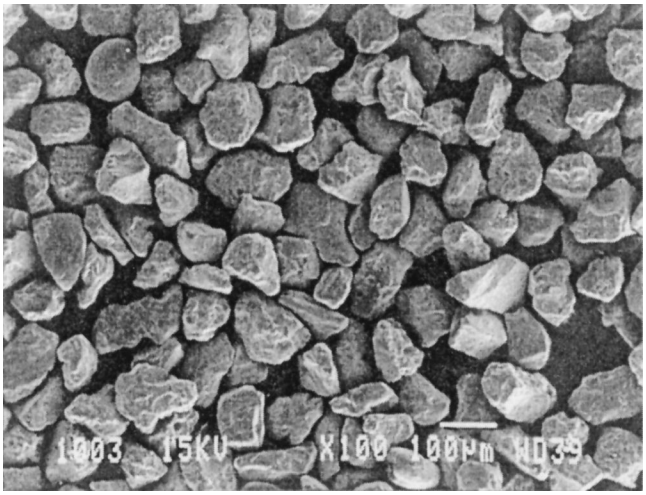

(*a*)

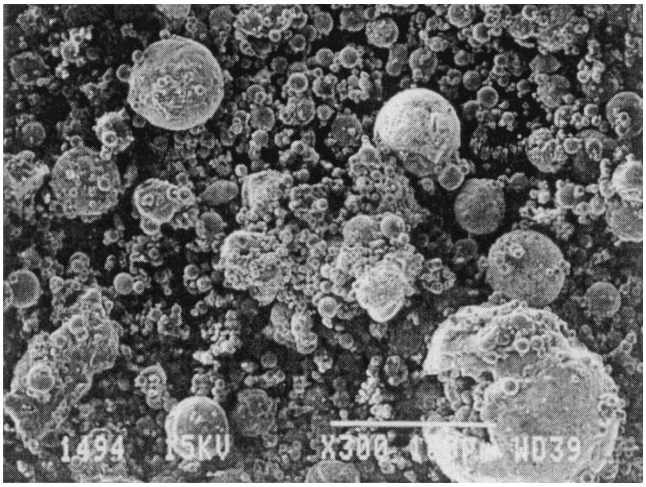

(*b*)

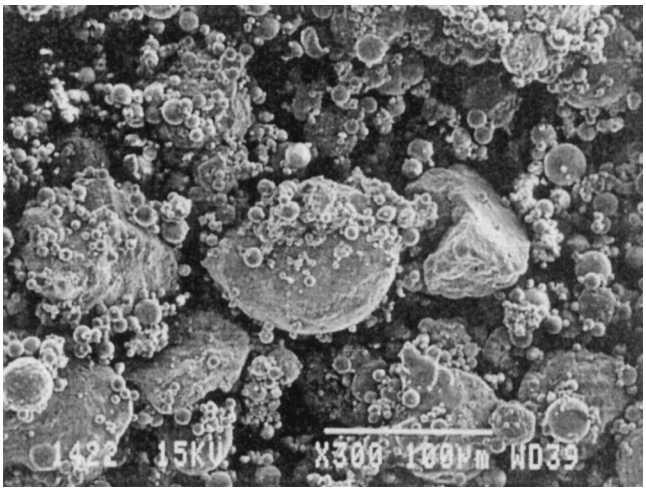

(*c*)

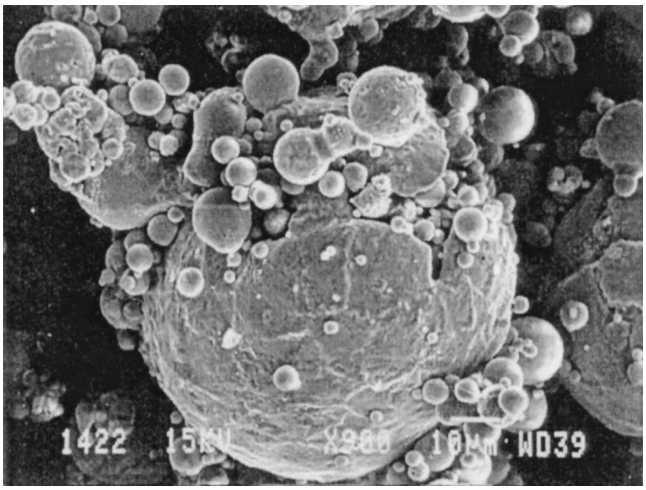

(*d*)

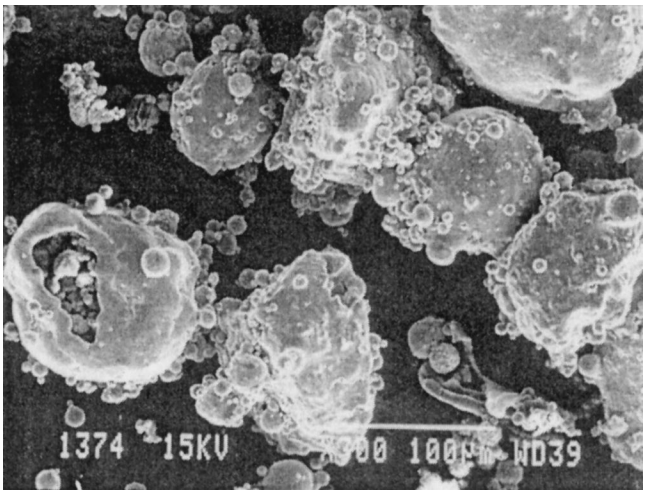

(*e*)

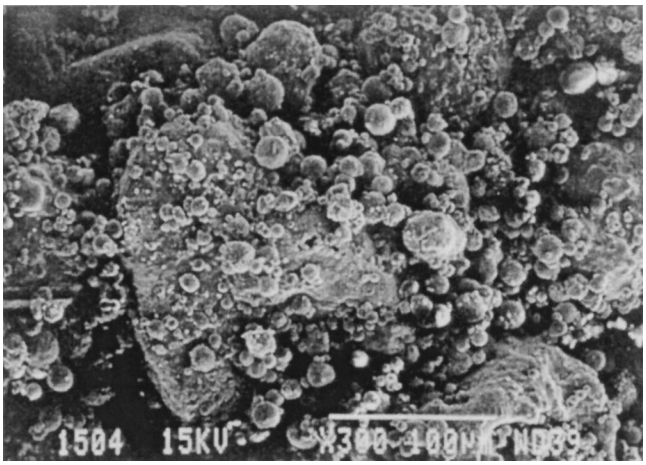

(*f*)

Fig. 12—Morphology of 72 pct particles: (*a*) fraction 74 to 105 μm; (*b*) receptacle sample, <37 μm, 0.33 kg O_2/kg matte, and 70 pct O_2; (*c*) receptacle sample, 37 to 74 μm, 0.25 kg O_2/kg matte, and 70 pct O_2; (*d*) cenosphere filled with fines, receptacle sample, 37 to 74 μm, 0.25 kg O_2/kg matte, and 70 pct O_2; (*e*) receptacle sample, 74 to 105 μm, 0.25 kg O_2/kg matte, and 70 pct O_2; (*f*) receptacle sample, 105 to 149 μm, 0.33 kg O_2/kg matte, and 70 pct O_2.

7. *Morphology*

The typical starting 72 pct matte particles were nonporous and angular in shape, as shown in Figure 12(a). Examination of the reacted particles of the receptacle samples indicated that the <37 μm fraction underwent extensive fragmentation, as shown in Figure 12(b). The angular shape of the

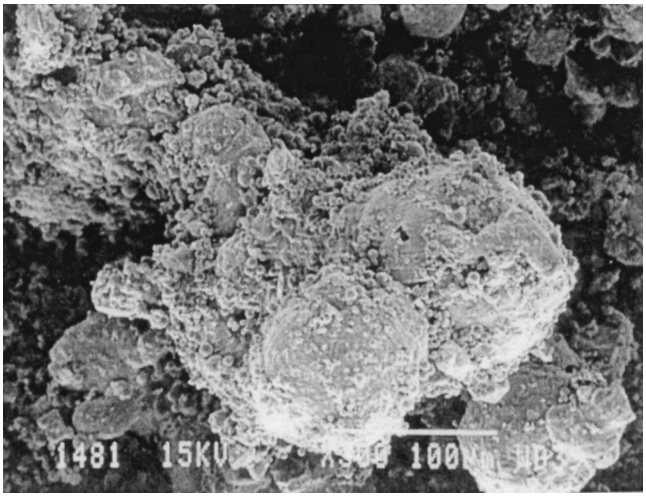

(*g*)

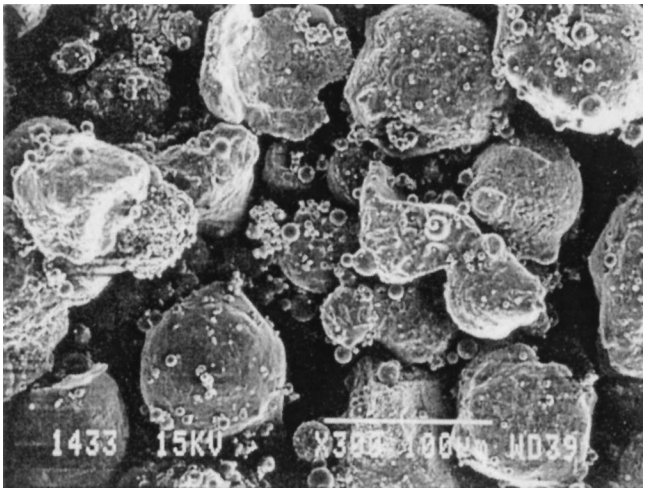

(*h*)

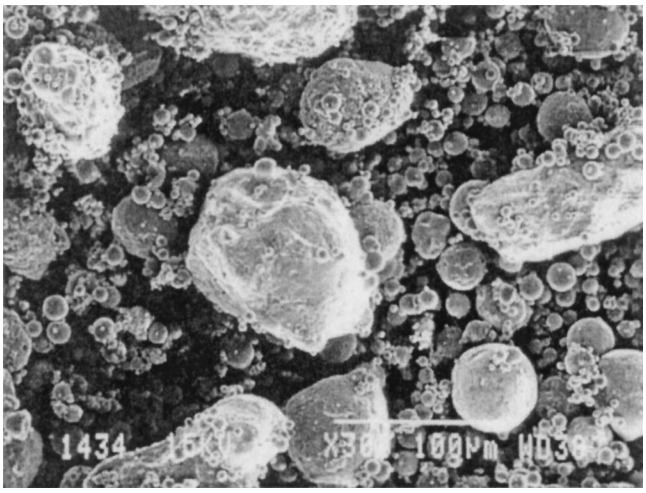

(*i*)

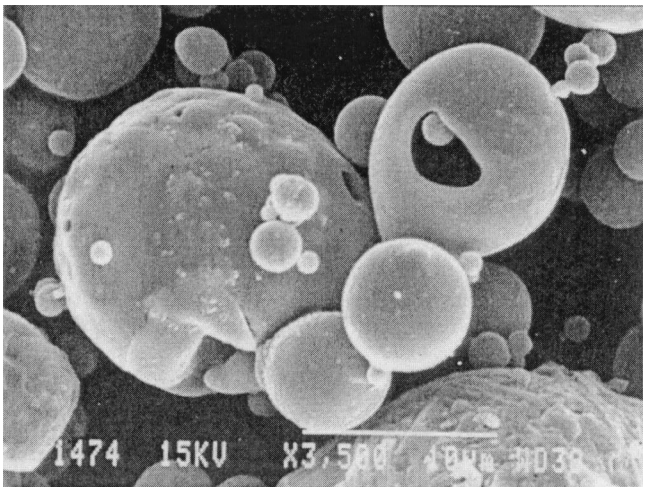

(*j*)

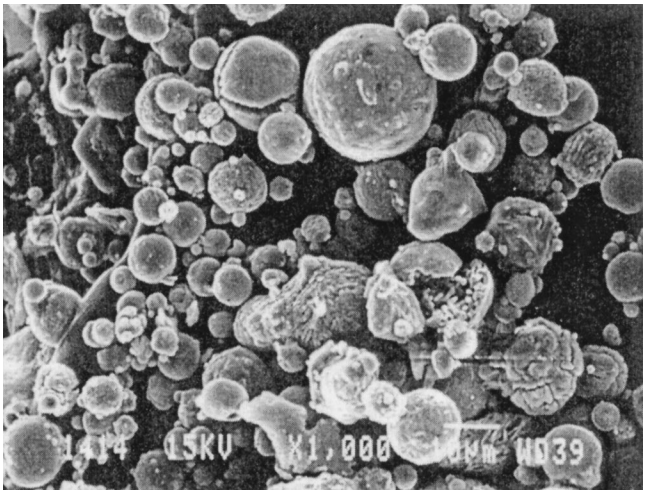

(*k*)

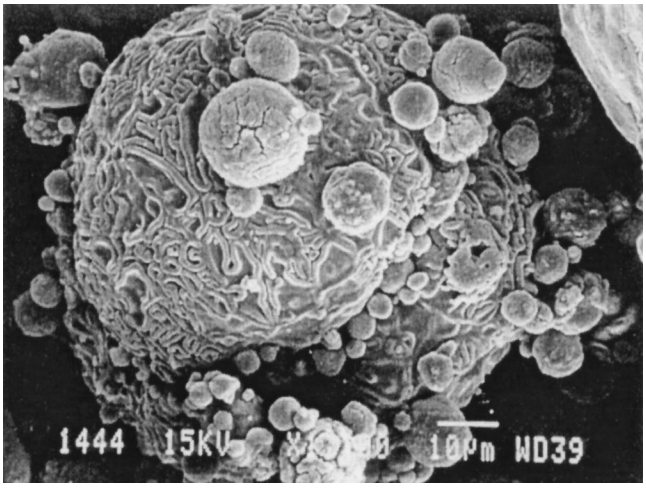

(*l*)

Fig. 12—Continued. Morphology of 72 pct particles: (*g*) agglomerate in probe sample collected 0.66 m below the burner tip, <37 μm, 0.25 kg O_2/kg matte, and 70 pct O_2; (*h*) probe sample collected 20 cm above the receptacle, 37 to 74 μm, 0.25 kg O_2/kg matte, and 100 pct O_2; (*i*) receptacle sample, 37 to 74 μm, 0.25 kg O_2/kg matte, and 100 pct O_2; (*j*) dust particles in receptacle sample, <37 μm, 0.33 kg O_2/kg matte, and 100 pct O_2; (*k*) dust particles in receptacle sample, 37 to 74 μm, 0.33 kg O_2/kg matte, 100 pct O_2; and (*l*) large particle covered by dust in receptacle sample, 105 to 149 μm, 0.25 kg O_2/kg matte, and 100 pct O_2.

feed particles disappeared, and particles turned into spheres in all experimental conditions. The larger spheres in the samples were covered with extremely fine round particles (1 to 10 μm in size). Agglomeration of the particles into bigger particles was observed, as well as the presence of cenospheres and hollow particles filled with fine particles (plerospheres). The diameter of some of the hollow particles was close to 100 μm; *i.e.*, particles significantly larger than the original feed particles were generated, which supports the hypothesis of particle expansion. The surfaces of the reacted fine particles, in general, were smooth, while the surfaces of the large particles were somewhat uneven and porous. Even crystalline surface structures were observed.

The 37 to 74 μm fraction fragmented significantly under all experimental conditions, as seen in Figure 12(c). Some angularly shaped particles still remained in the receptacle samples, even though most of the particles became round. The surfaces of the finest particles ($<$10 μm), in general, were smooth, while larger particles had uneven surfaces. Porous, cracked, and scaling surface structures were also observed. Few agglomerates were found among the cenospheres, which tended to have a thick crust and numerous round, fine particles inside them, as shown in Figure 12(d). Irregularly shaped hollow particles were also found.

Particles from the receptacle samples of the 74 to 105 μm fraction retained their original angular shape, to a greater extent, better than the two finer fractions. Some agglomerates, consisting of both the original-size particles or fine fragmented particles, were found in the samples. When the oxygen-to-matte ratio was increased to 0.33 kg O_2/kg matte, more large particles became round, and the amount of fine particles surrounding the 100 μm particles increased. Hollow particles and cenospheres were also found. Some of them had a thick crust with gas blow holes in them, while others had thinner crusts partially torn away, exposing a large amount of fines inside them. The surfaces of both the large and fine particles were uneven, with pores and cracks in them. Figure 12(e) shows typical reacted particles of the 74 to 105 μm fraction.

Samples from the 105 to 149 μm fraction consisted mainly of large, round particles and small spheres. Both the large and fine particles had uneven surfaces, but the fines had deeper cracks on the surface. A few fine particles were attached to the surface of some large particles, forming agglomerates. The size of the agglomerates did not differ significantly from the original particle size. Cenospheres and irregularly shaped hollow particles were formed during the oxidation. Some were empty, with gas holes in the crust, while others still had fine particles inside them. Reacted matte particles of the 105 to 149 μm fraction are presented in Figure 12(f).

The SEM micrographs of the two highest probe samples along the centerline (0.66 and 0.86 m from the burner tip) and of those of the receptacle samples showed no significant difference in the particle appearance. In some cases, in which the fractional conversion of the probe sample differed from that of the receptacle sample, a difference in the particle-size distribution could be seen. When the fractional conversion and sulfur-removal values were higher, the extent of fragmentation was also higher. On the other hand, agglomeration was more often observed in probe samples than in receptacle samples. A typical agglomerate is shown in Figure 12(g).

In some experiments, particle samples were collected with the probe at 20 cm above the receptacle. A clear difference between the probe and receptacle samples could be seen, including the unexpected result that the fractional conversion of the probe sample reached significantly lower values than that of the receptacle sample. In such cases, the probe sample consisted mainly of coarse, round particles together with numerous fine spheres. Probe and receptacle samples are shown in Figure 12(h) and (i). No significant differences in sulfur removal between the samples shown in these figures were determined.

The morphology of dust particles in the receptacle samples differed from one particle to another. Some of the fine particles ($<$20 μm) had a smooth surface. Some of them turned into cenospheres and had small gas blow holes in them, as can be seen in Figure 12(j). Most of the dust particles had uneven and cracked surfaces, as shown in Figures 12(k) and (l).

Overall, the 72 pct matte particles generated a large amount of fine spheres. The coarser fractions had more angular particles remaining in the samples. Fine particles that melted thoroughly turned into spheres with a smooth surface. Large particles, on the other hand, had a more uneven surface with pores.

Large, hollow, irregularly shaped particles and cenospheres were observed. Reacted particles had gas blow holes on the surface, or fine particles inside them, regardless of their original particle size. However, the likelihood of hollow particles to be spheres was greater with finer feed fractions than with coarser feed particles. A thin oxide layer containing some iron oxides was formed on the surface. Cenospheres, in this study, were likely to form due to the buildup of gas pressure inside the particle, while the surface tension of the molten particle was enough to resist immediate explosion.

Agglomerates were formed by the collision of partially or fully molten particles at high temperatures. The amount of agglomerates decreased with increasing initial particle size. The size of some agglomerates obtained with the $<$37 μm fraction more than doubled the size of the initial particle size. The size of the agglomerates obtained with the coarse-feed fractions was not substantially larger than the initial particle size. Possibly, the agglomerates were formed either in the probe or in the receptacle before the particles were quenched. Because the particle loading in the furnace was low (less than 0.01 pct by volume), particle-particle collisions in the reaction chamber were not likely.

Large particles underwent partial oxidation, while smaller particles, in general, reacted further. A thin iron oxide/copper oxide layer was formed around the large particles. Large particles that had reacted further had an iron oxide rim deep in the particle around the core. The porosity of this rim decreased for smaller particles. Iron oxide rims and elemental copper inclusions were more common among fine particles.

8. *Mineralogy*

The feed matte particles were found to be relatively homogeneous, containing a few inclusions consisting of elemental copper.

The 74 to 105 and 105 to 149 μm fractions underwent

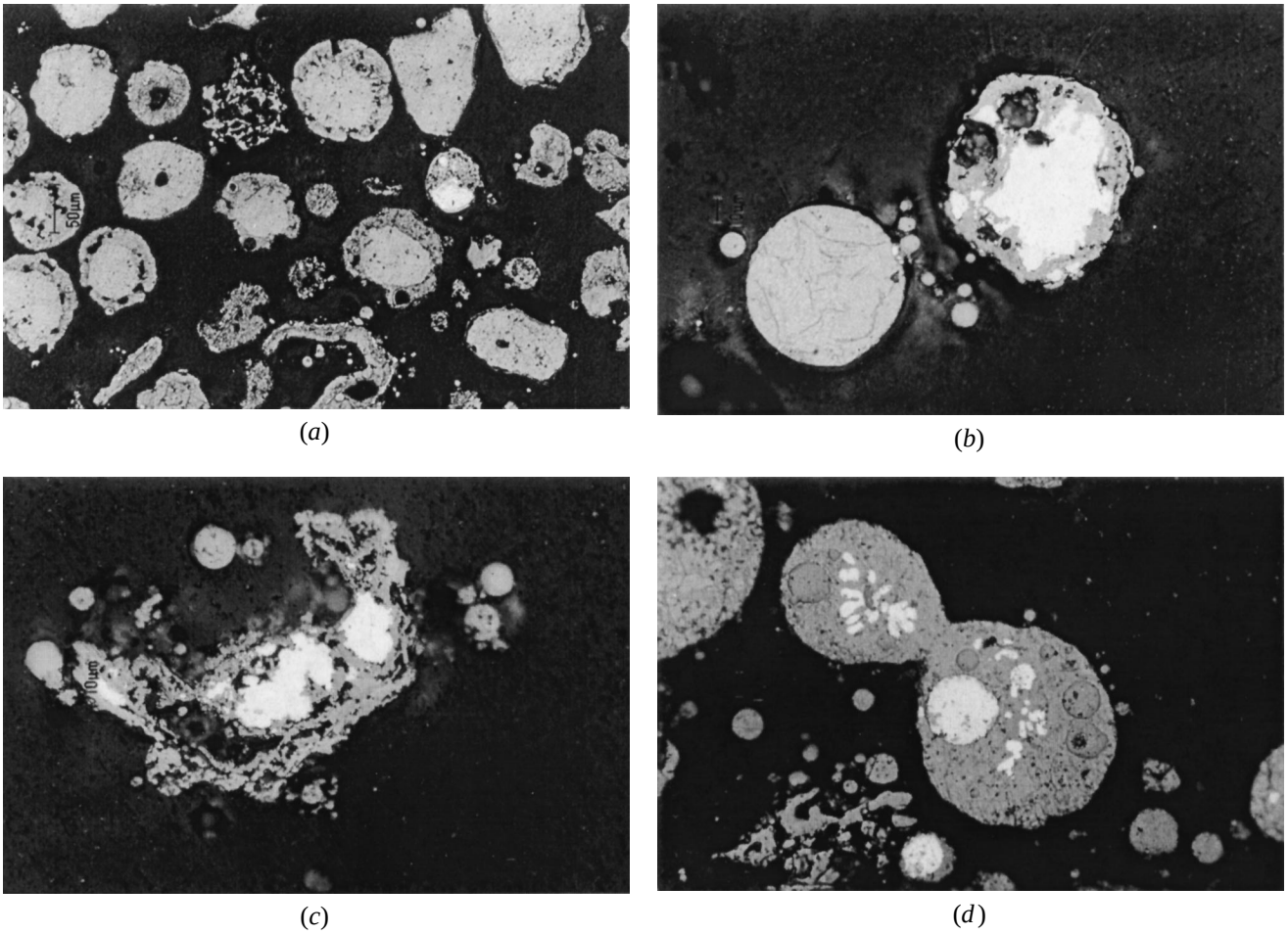

(*a*) (*b*) (*c*) (*d*)

Fig. 13—Mineralogy of 72 pct matte particles: (*a*) oxidized particles in receptacle sample, 74 to 105 μm, 0.25 kg O_2/kg matte, and 100 pct O_2; (*b*) a dendritic particle together with a fully melted particle, receptacle sample, 74 to 105 μm, 0.33 kg O_2/kg matte, and 70 pct O_2; (*c*) an extensively oxidized cenosphere showing elemental copper surrounded by copper oxides and Cu-S-O phase, receptacle sample, 105 to 149 μm, 0.33 kg O_2/kg matte, and 100 pct O_2; and (*d*) an irregular iron oxide phase and elemental copper inclusions inside an oxidized particle, receptacle sample, 37 to 74 μm, 0.33 kg O_2/kg matte, and 100 pct O_2.

partial oxidation under all experimental conditions. The surface consisted of iron oxides, copper oxides, and copper sulfides, which were detached from the core by a porous rim. The core of partially molten particles consisted of copper sulfide. When the reactions proceeded further, the pores became larger, and an iron oxide rim was formed between the core and the partially oxidized copper sulfide surface. The outer oxidized surface of some particles contained little sulfur. The oxidized surface, in general, was thicker in particles from the 74 to 105 μm fraction than in those from the 105 to 149 μm fraction. A general view of oxidized particles of the 74 to 105 μm fraction is shown in Figure 13(a).

Fully melted particles consisted of dendritic copper sulfide and an interdendritic Cu-S-O phase. Elemental copper and copper oxide phases were formed in further-oxidized particles. This is shown in Figure 13(b). The detection of elemental copper was not restricted to the particle core; elemental copper was also found on the particle surface. Many of the particles showed large holes; *i.e.*, hollow particles and cenospheres were formed. An extensively reacted hollow particle is shown in Figure 13(c).

The small particles reacted further than the coarse particles. The oxide rim in the reacted particles of the 37 to 74 μm fraction was thicker and more porous than that in the coarse particles, as seen in Figure 13(d). Irregular iron oxide grains were formed, as well as elemental copper. Copper oxides were also formed. The particles of the finest fraction were oxidized more extensively. Finer particles that melted completely consisted of copper sulfides and its various oxidized forms (Cu-S-O). Copper oxide and a substantial amount of elemental copper precipitates were detected. The finest fraction had more elemental copper than other fractions.

The dust particles ($<$20 μm in size) were mainly copper oxide particles. (Cu_2O) with some oxidized iron. Practically no sulfur was detected in these particles. This suggests that dust was generated by fragmentation of large, extensively oxidized particles or that small sulfide particles were produced by fragmentation or pinching off from large particles and were rapidly oxidized.

B. *Low-Grade (58 pct) Matte Feed*

All the experiments with the 58 pct matte were conducted with the stoichiometric amount of oxygen, as indicated in Table I. Thus, the effect of the oxygen-to-matte ratio was not tested in these experiments.

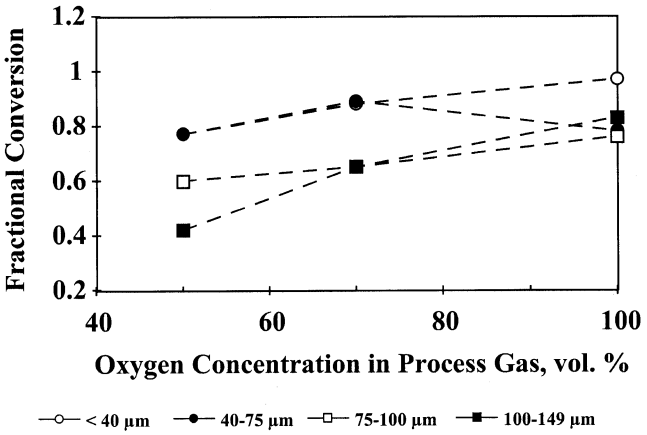

Fig. 14—Fractional conversion of the receptacle samples, 58 pct matte particles; all runs at 0.3 kg O_2/kg matte.

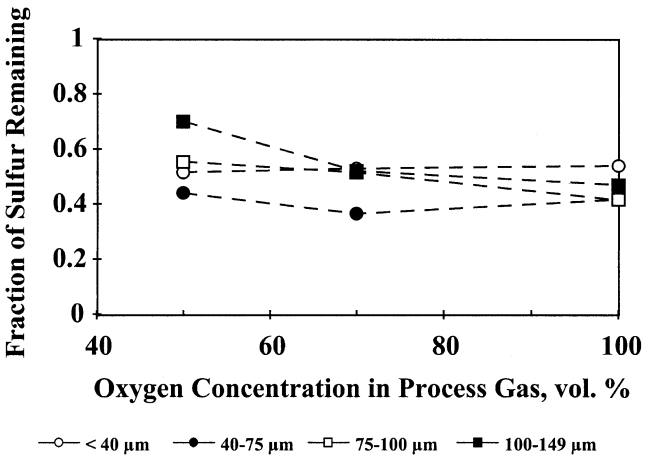

Fig. 15—Fraction of sulfur remaining in the receptacle samples, 58 pct matte particles; all runs at 0.3 kg O_2/kg matte.

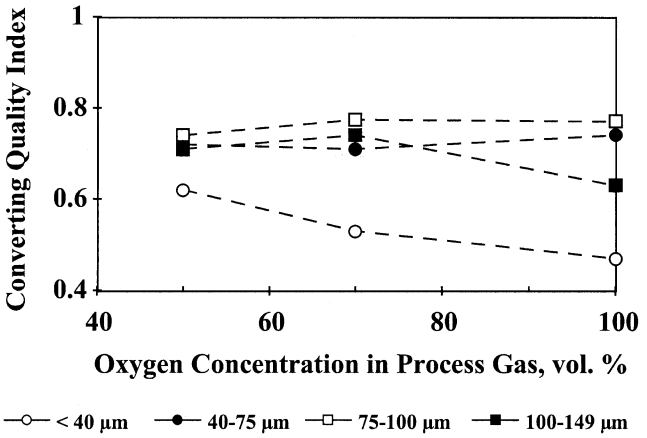

Fig. 16—Converting quality index of the receptacle samples, 58 pct matte particles; all runs at 0.3 kg O_2/kg matte.

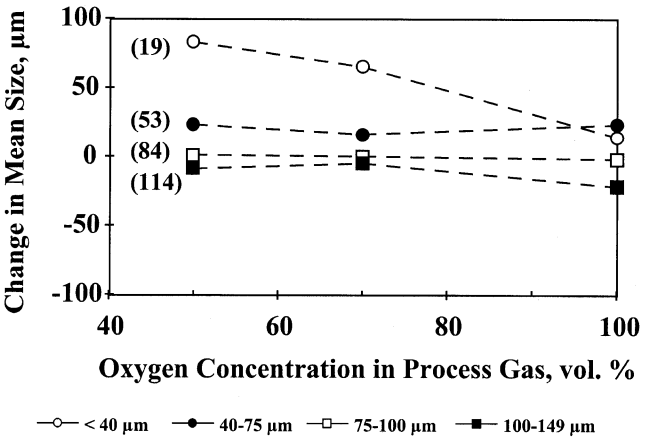

Fig. 17—Change in mean size between receptacle and feed particles, 58 pct matte; values in parentheses indicate the mean size of the feed, in μm; all runs at 0.3 kg O_2/kg matte.

1. *Fractional conversion*

Overall, the 58 pct matte particles reacted more evenly than the 72 pct matte particles. This is shown in Figure 14. The fractional conversion did not exceed the value of unity in any experiment. In general, small particles reacted further than large particles. Similarly to the results obtained with the 72 pct matte, no effect of oxygen content was observed within the range from 70 to 100 pct. As stated earlier, this may be explained by the blockage of the pores in the oxide shell when pure oxygen was used and by the effect of the hydrodynamics, which promoted a better mixing with 70 pct oxygen than with pure oxygen. Overall, the fractional conversion varied between 0.4 and 0.9. The estimated oxygen consumption computed from Eq. [5] varied between 40 and 84 pct.

2. *Sulfur removal*

The trends for sulfur removal were similar to those for fractional conversion and are shown in Figure 15. The removal of sulfur varied between 30 and 60 pct for all feed fractions studied.

3. *Converting-quality index*

Figure 16 shows the converting-quality index for the 58 pct matte samples. The converting-quality index was relatively insensitive to particle size when the feed size was greater than 40 μm. The finest particles, <40 μm, achieved the poorest quality of conversion in all the experiments. The oxygen concentration, in general, did not play a significant role. The quality of the conversion achieved by the 58 pct matte particles was higher (0.6 to 0.75) than that achieved by the 72 pct matte particles (0.4 to 0.7). Thus, the 58 pct matte particles reacted more evenly in the reaction shaft than the 72 pct matte particles under all experimental conditions.

These discrepancies suggest a significant difference in the reaction behavior of the two matte samples, which is attributable to the differences in iron and sulfur contents. The 58 pct matte contains more iron and sulfur than the 72 pct matte. Upon oxidation, the 58 pct matte particles produced a higher amount of iron oxides, which prevented fragmentation and decreased the overall oxidation rate.

4. *Copper-to-iron atomic ratio*

Little variation in the Cu/Fe atomic ratio was observed in the experiments with the 58 pct matte, suggesting that little copper volatilization occurred.

5. *Mean size*

Figure 17 shows the change in mean particle size computed by Eq. [5]. The results are substantially different from those observed in the 72 pct matte. The finest particles, <40

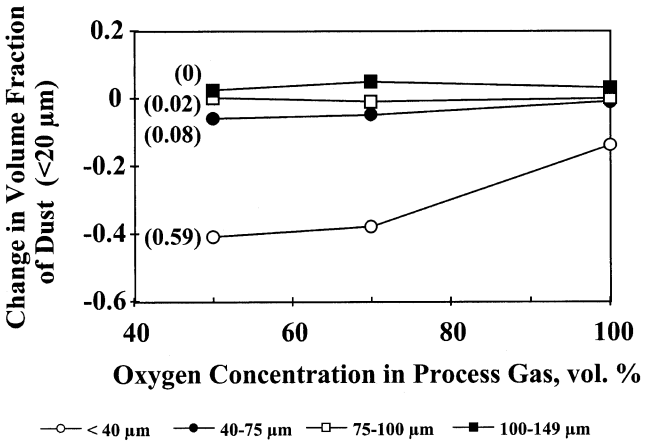

Fig. 18—Change in dust content between receptacle and feed particles, 58 pct matte; values in parentheses indicate the volume fraction of dust particles (<20 μm) in the feed; all runs at 0.3 kg O_2/kg matte.

μm in size, became larger with a low oxygen concentration, possibly due to particle expansion, but remained similar in size with pure oxygen. As the mean size of the feed particles increased, they began to fragment. The largest increase in the mean size was about 80 μm; this occurred for the <40 μm fraction. The largest decrease in the mean size was about 25 μm, which occurred for the 100 to 149 μm fraction. The oxygen concentration did not play a major role in changing the particle size.

6. *Dust generation*

In contrast with the results obtained with the 72 pct matte, practically no dust was produced by the 58 pct matte (Figure 18). The finest fraction, <40 μm, lost dust particles due to particle expansion. The generation of dust was not affected by the oxygen content of the process gas.

7. *Morphology*

Figure 19(a) shows an SEM image of typical 58 pct matte particles. The <40 μm fraction consisted of many fine and angularly shaped particles, many of which were approximately 10 μm in size. Some large chunks were among several fine particles.

The 40 to 75 μm fraction was much coarser, but contained a significant amount of fines. The particles in these fractions appeared to be angular, but somewhat flat. The 75 to 100 and 100 to 149 μm fractions were relatively free of fines, and the particle shapes and sizes were more uniform in these fractions.

The appearance of reacted samples from the <40 μm fraction differed significantly from that of the feed, as seen in Figure 19(b). The shape of many of the fines (<10 μm in size) changed; the angular shape became less apparent as particles became rounder. Several large and somewhat round particles appeared in the receptacle samples. The size of these particles reached over 100 μm, significantly larger than the original feed particles. They were typically covered by several fine particles of approximately 10 μm in size. A few agglomerates consisting of several large spheres and a few cenospheres were found in the samples. The agglomerates were probably formed in the receptacle moments before the particles were quenched.

The number of large particles in the samples was seen to increase with decreasing oxygen concentration in the process gas; thus, 50 pct oxygen produced the greatest number of large particles, and pure oxygen produced the fewest large particles.

The reacted particles of the 40 to 75 μm fraction were rounder and more uniform in size than those of the <40 μm fraction, as shown in Figure 19(c). Several spheres were found in the samples; the largest particles observed were approximately 120 μm in size. One of these large particles is shown in Figure 19(d). They were covered by several small spheres of approximately 10 μm in size and had uneven surfaces. Few of the coarse particles appeared to be agglomerates, which supports the hypothesis of particle expansion. In general, the number of burst particles and particles with fines inside them (plerospheres) was small.

Receptacle samples from the 75 to 100 and 100 to 149 μm fractions had almost no fines. Angular edges of the particles became smoother and the particles became rounder. Typical examples of the reacted particles from these size fractions are shown in Figures 19(e) and (f), respectively. As can be seen from Figure 19(g), some agglomerates were also formed with the 75 to 100 μm fraction. As the oxygen content of the process gas became higher, the particles of these two size fractions became rounder. Thus, at a 70 pct oxygen concentration, a few burst particles and particles with fines inside them were observed. However, when the oxygen concentration was increased to 100 pct, the particle appearance changed greatly, and severe fragmentation was observed, as shown in Figure 19(h). Most of the particles obtained at a high oxygen concentration were spheres in the range of 1 to 150 μm in size.

Hollow particles were also observed. Hollow burst particles are shown in Figures 19(i) and (j). Typically, the crust of the hollow particles was relatively thick, and the hollow particle was either filled with or covered by numerous fine, spherical particles, but the presence of thin-shell cenospheres was scarce. Bubble formations, like that shown in Figure 19(k), were typically located near the edge of the particle, not in the core. This suggests that the internal pressure, probably caused by generation of sulfur dioxide gas, was easily released from the particles.

Overall, the 58 pct matte particles became rounder upon oxidation. Simultaneously, the size of some of the particles increased significantly, due to internal gas generation and spheroidization by melting. As an example, particles of 100 μm in size were observed in samples from the finest size fraction, <40 μm. A few of the largest particles appeared to be agglomerates, which were probably formed in the receptacle or the probe before quenching took place. The number of burst particles and those with fines inside them was relatively small at low oxygen concentrations, which suggests that fragmentation was not severe when the oxidation reactions were slow. An increase in the number of burst particles was observed when pure oxygen was used, suggesting increasing particle fragmentation when the oxidation reactions were fast.

8. *Mineralogy*

Mineralogical examination of the reacted particles indicated that chalcocite (Cu_2S) and digenite (Cu_9S_5) were the most abundant phases in the particles. They were commonly intergrown in a very fine-grained texture. The amount of bornite (Cu_5FeS_4) in the reacted particles was less than the

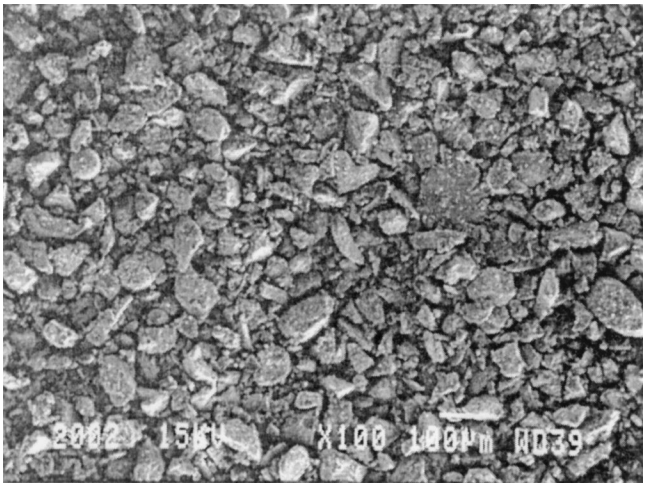

(*a*)

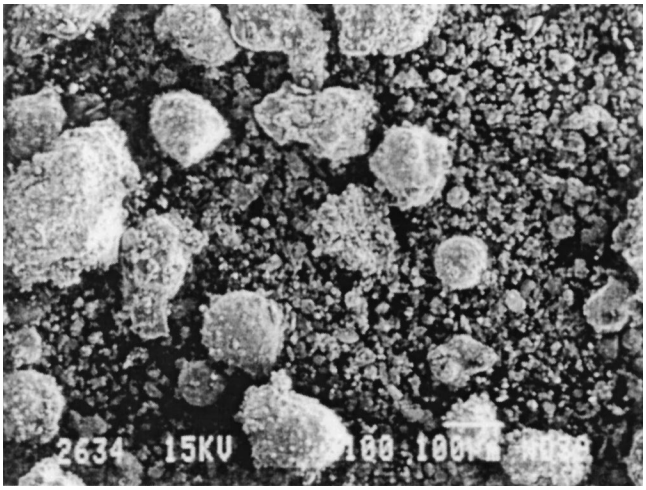

(*b*)

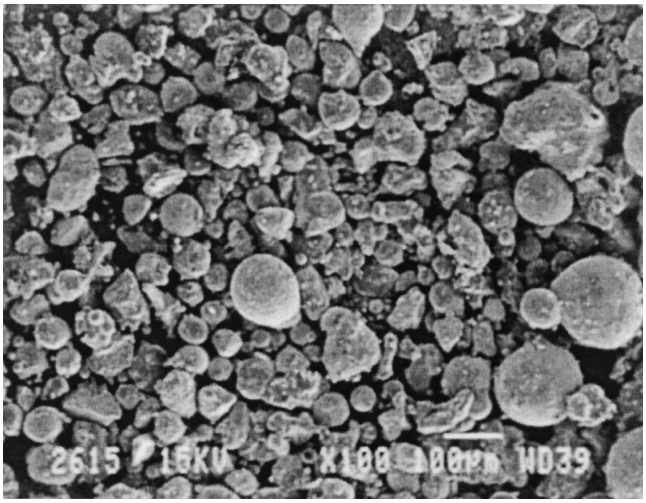

(*c*)

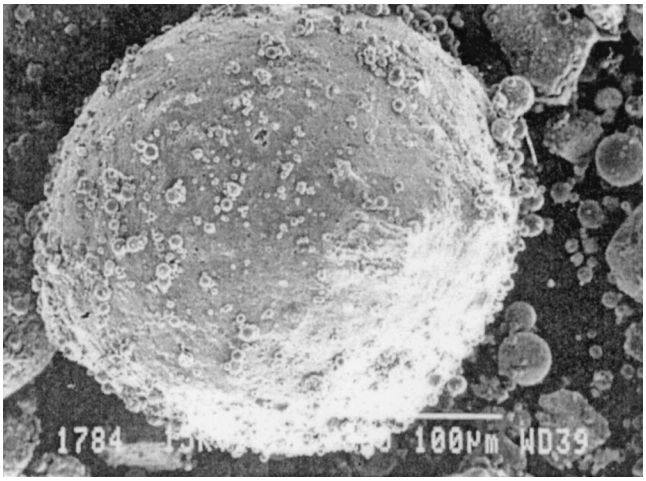

(*d*)

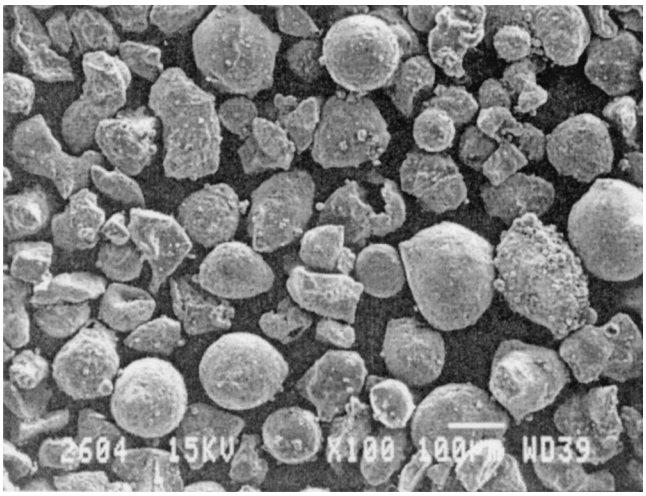

(*e*)

(*f*)

Fig. 19—Morphology of 58 pct particles: (*a*) original matte particles, and fraction 40 to 75 μm; (*b*) receptacle sample, $<$40 μm, and 70 pct O_2; (*c*) receptacle sample, 40 to 75 μm, and 70 pct O_2; (*d*) large reacted particle, receptacle sample, 40 to 75 μm, and 100 pct O_2; (*e*) receptacle sample, 75 to 100 μm, and 70 pct O_2; (*f*) receptacle sample, 100 to 149 μm, and 70 pct O_2.

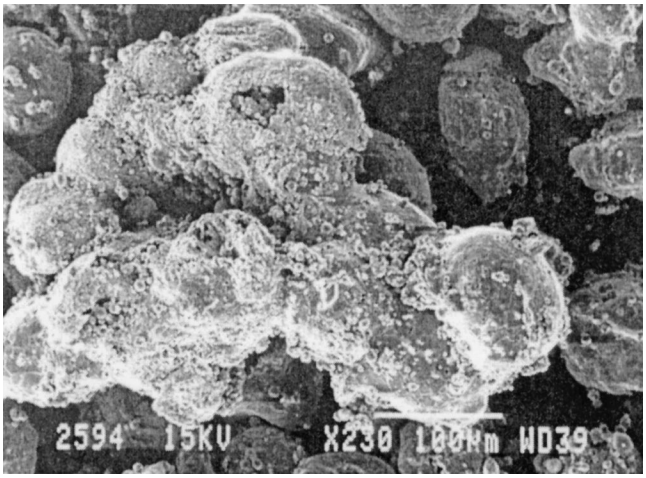

(*g*)

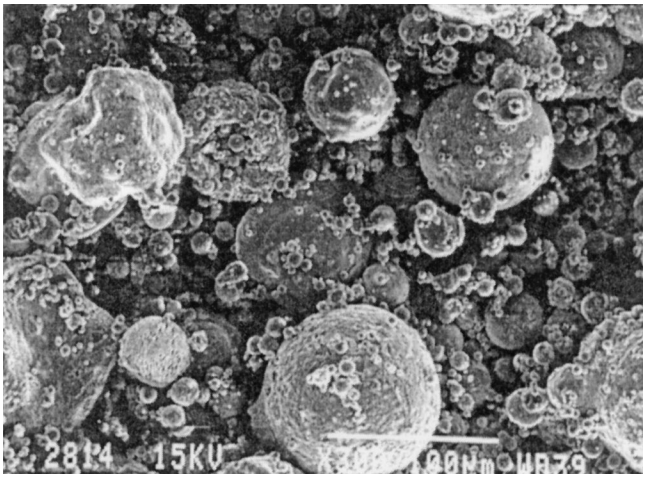

(*h*)

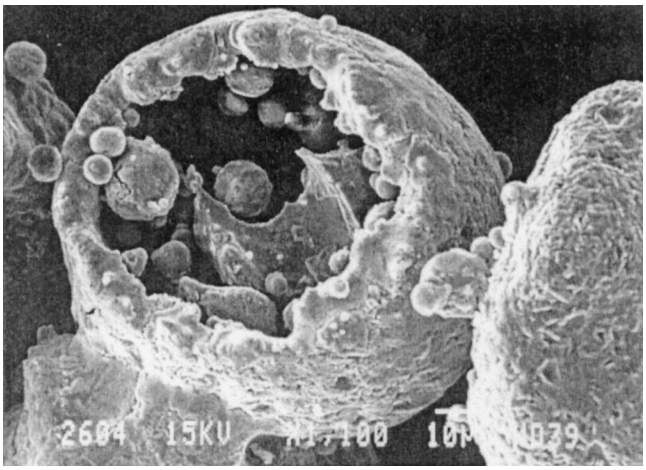

(*i*)

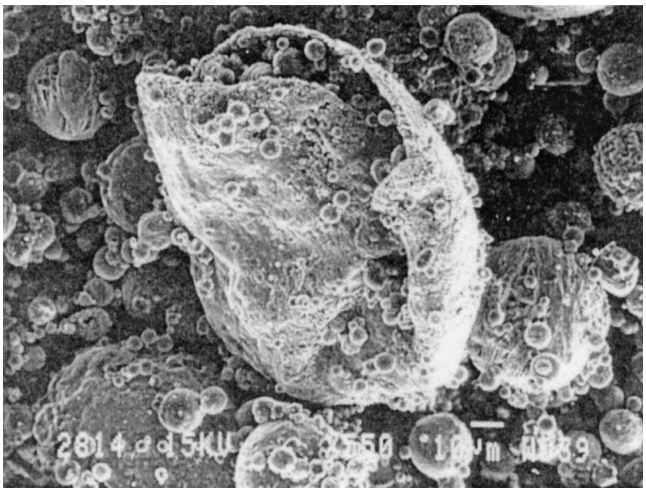

(*j*)

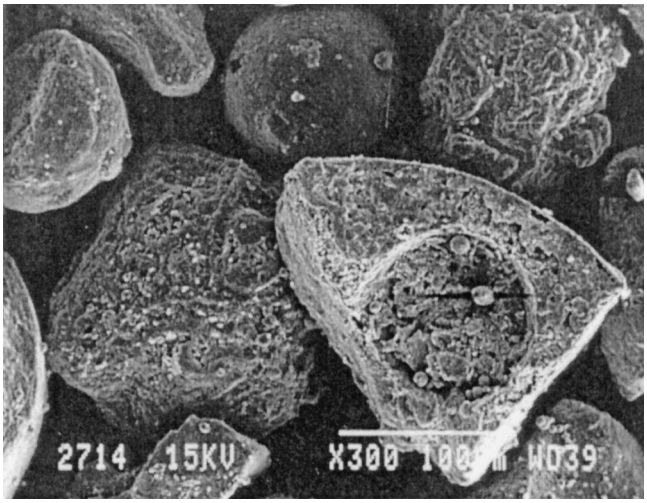

(*k*)

Fig. 19—Continued. Morphology of 58 pct particles: (*g*) agglomerate consisting of spheres, receptacle sample, 75 to 100 μm, and 70 pct O_2; (*h*) receptacle sample, 100 to 149 μm, and 100 pct O_2; (*i*) hollow sphere filled with fines, receptacle sample, 75 to 100 μm, and 70 pct O_2; (*j*) hollow collapsed particle, receptacle sample, 100 to 149 μm, and 100 pct O_2; and (*k*) a bubble formed inside a particle, receptacle sample, 100 to 149 μm, and 50 pct O_2.

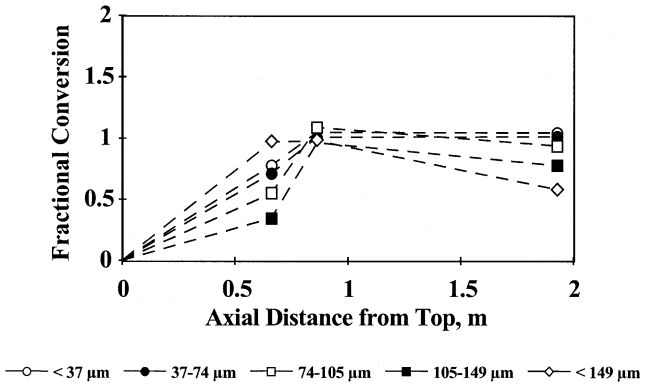

Fig. 20—Fractional conversion values along the centerline and receptacle, 72 pct matte particles; experimental conditions: 70 pct oxygen, and 0.25 kg O_2/kg matte.

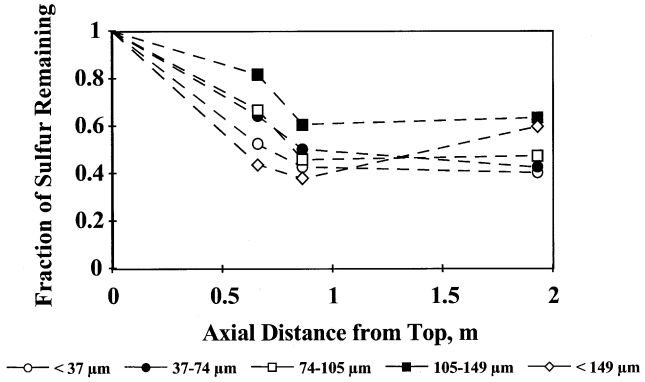

Fig. 21—Sulfur remaining values along the centerline and receptacle, 72 pct matte particles; experimental conditions: 70 pct oxygen content, and 0.25 kg O_2/kg matte.

amounts of chalcocite and digenite. Inclusions of elemental copper as well as tenorite (CuO) were also detected in the samples. Iron oxide layers were not observed around the particles.

C. *The Role of Hydrodynamics of the Reaction Path*

The results of the probe samples collected along the centerline of the reaction chamber are discussed in detail in Reference 15. The most relevant finding was related to the nature of the hydrodynamic conditions attained in the experimental setup.

The analysis of the probe samples suggested that the reaction conditions in the furnace were not uniform, *i.e.*, that particles in the shaft faced different reaction conditions as they traveled through the shaft. Figures 20 through 22 represent examples of the results. Figure 20 indicates that the fractional conversion increases with axial distance from the top. This is an expected trend, since particles undergo oxidation as they flow downward in the shaft. However, it is noted that the fractional conversion values in the receptacle samples were, in general, lower than those of the probe samples collected at 0.86 m below the burner tip. These apparently contradictory results can be explained by recognizing that probe samples represented local conditions along the centerline, whereas the receptacle samples represented

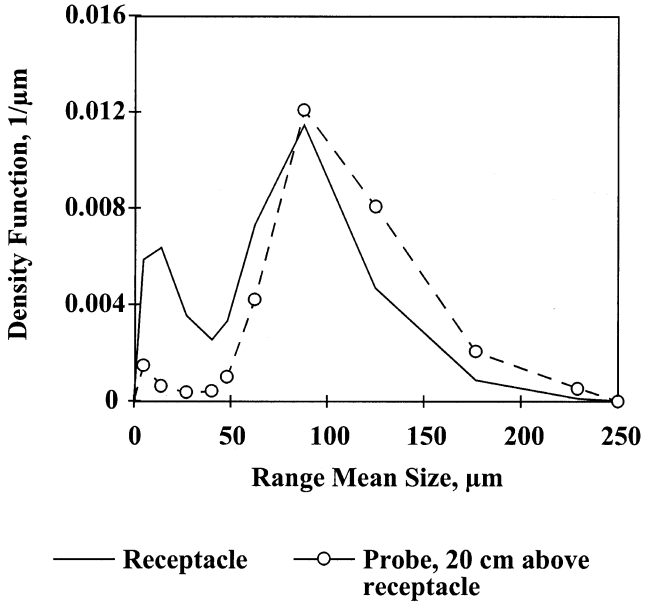

Fig. 22—Particle size distribution by volume of the receptacle and probe samples collected 20 cm above the receptacle, feed fraction: 74 to 105 μm of the 72 pct matte; experimental conditions: 0.25 kg O_2/kg matte, and 100 pct O_2.

the collection of all the particles that reached the bottom following different trajectories along the reaction shaft. Therefore, the receptacle samples contained both highly oxidized and partially oxidized particles. The degree of oxidation of the particles collected in the receptacle depended upon the reaction path followed by each particle in the shaft. A direct implication of these observations is that oxygen consumption in the shaft was not even, but varied with location in the furnace. That is, the reactor did not behave as a plug-flow reactor.

On the other hand, the values of sulfur remaining in the receptacle samples of the 72 pct matte (Figure 21) in general followed the trend observed in the probe samples. In many cases, the sulfur remaining in the probe samples collected at 0.86 m from the top did not differ substantially from the sulfur remaining in the receptacle samples. In contrast with the previous discussion, this suggests that sulfur was removed more evenly in the reaction shaft. That is, the reactions leading to the removal of sulfur were mostly confined within 0.86 m from the burner tip, but the oxygen consumption varied more significantly with location in the furnace, as Figure 20 suggests. If any reactions took place in the shaft beyond 0.86 m from the top, they were predominantly overoxidation reactions, not sulfur-oxidation reactions. The results in Figures 20 and 21 point out the relevance of tracking both the fractional conversion and sulfur removal during the oxidation of copper matte particles.

In some runs with the 72 pct matte, probe samples were collected 1.72 m below the burner tip, which was approximately 20 cm above the receptacle. The particle-size distribution of one of these samples is shown in Figure 22 and is compared with the particle-size distribution obtained in the receptacle. The probe sample contained a significantly lower volume of fine particles ($<$50 μm in size) than the receptacle samples. Also, the volume of large particles ($>$100 μm in size) in the probe samples was larger than in

the receptacle samples. At 20 cm above the receptacle, no further reactions were assumed to take place in the particles. The reaction flame occurred in the upper portion of the shaft, and the furnace walls in the receptacle area were water cooled, thus providing a quenching effect to the particles. Thus, it is unlikely that the differences shown in Figure 22 were due to chemical reactions or physical transformations of the falling particles. Rather, it is more likely that the sampling probe mostly collected coarse, heavy particles falling near the centerline, whereas fine, light particles reached the bottom following a less direct trajectory. Thus, the interpretation of Figure 22 also supports the importance of the hydrodynamic conditions in the furnace.

D. *Other Observations Regarding Dust Generation*

Exploratory tests not detailed in this article showed that dust generation in this system could also be affected by the burner configuration used in the experiments.[15] When a single-entry type of burner was used, *i.e.*, particles and gas were fed together through the primary stream, a higher amount of dust was generated than with the six-jet entry system shown in Figure 4. The different degree of mixing promoted by each type of burner design, *i.e.*, the hydrodynamic conditions, may be responsible for this observation. These results point out the role that burner design may play in the performance of an industrial flash-converting operation and indicate the need for further investigation of the effect of fluid dynamics on dust generation.

E. *Qualitative Model of Particle Fragmentation*

The fragmentation of copper matte particles is the main factor responsible for dust generation during the oxidation. The model discussed in this section intends to provide an interpretation of most of the physical changes observed in the particles.

The fragmentation of sulfide particles is a complex phenomenon in which different processes participate. There seems to be no unique mechanism by which sulfide particles fragment when they react in an oxidizing atmosphere. Differences in particle composition and reaction conditions strongly affect the path followed by individual particles during fragmentation.

The model discussed in this section is based on the reaction path originally proposed by Kim and Themelis[8] and further modified by Jokilaakso *et al.*[22] A thorough review of the fragmentation mechanisms of sulfide particles, coal particles, and metal droplets has been presented by Riihilahti.[19]

The model is shown schematically in Figure 23. The oxidation starts at the particle surface. Because of its higher reactivity, the iron sulfide in the matte is oxidized first. Upon ignition, the unreacted sulfide core melts, while the particle surface consists of a highly viscous or porous solid mixture of oxides and sulfides. Due to the oxidation of sulfur, sulfur dioxide is formed within the particle, creating small bubbles that grow as the reactions proceed. The increase in internal gas pressure as a result of the gas generation causes the particles to bloat into larger spheres.

The fragmentation of copper matte particles possibly takes place by molten material from the core being pushed out of the particle through the pores of the oxide layer. The molten material forms small spheres which detach from the surface of the larger particle. The displacement of the molten sulfides within the particle expands the gas bubbles inside the core, reducing the internal vapor pressure.

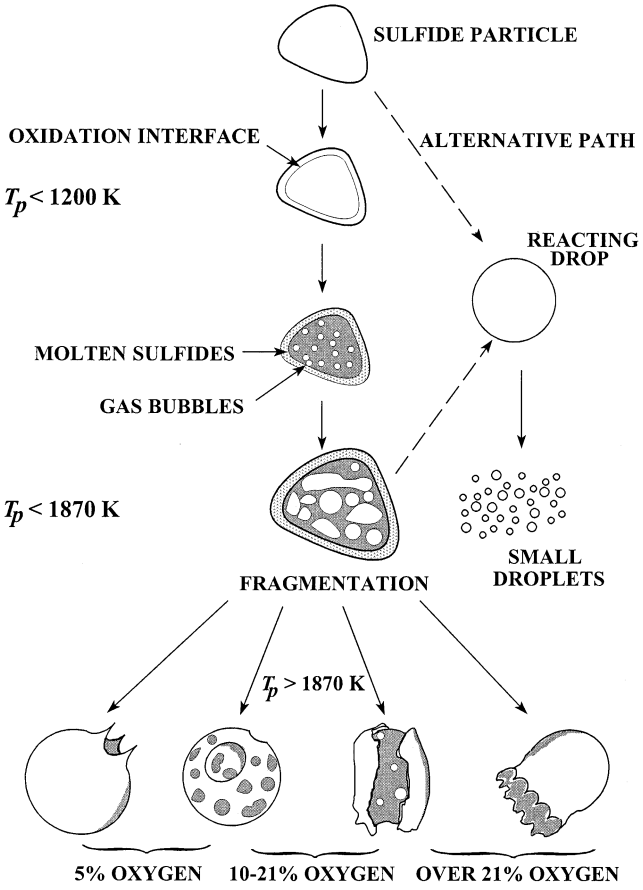

Fig. 23—Qualitative model of particle fragmentation; adapted from Kim and Themelis[8] and Jokilaakso *et al.*[22]

The molten material being pushed out through the pores can also block the pores. This builds up pressure inside the particle. When the internal gas pressure within the molten core exceeds the surface tension of the surface, the particle fragments.

The evolution of gas can result in the ejection of molten material in a finely divided form through the ruptured crust, leaving a hollow shell. Gas evolution can also detach the crust from the core, creating crust fragments. In some cases, the internal gas pressure may cause the crust to explode into pieces and the molten core to be discharged as small droplets. If the particle walls expand sufficiently due to the pressure increase, they become thin. This enables the pressure to be relieved by small holes on the particle surface. This mechanism produces cenospheres and small fragments, or just particles with gas blow holes.

The resistance of the solid crust to fragmentation is related to its iron content. A particle crust made up of sulfides and oxides of copper has a lower melting point than a crust made up of pure iron oxides and, thus, has a lower resistance to fragmentation. Iron oxides seem to act as a viscous glue, holding the particle together and preventing fragmentation. This may explain why the 72 pct matte particles appeared to explode, whereas the 58 pct matte particles were more resistant to fragmentation.

When the 58 pct matte particles fragmented, they seemed to eject molten material after the initial expansion during the oxidation. Droplets could also be produced by materials that pinch off from larger molten particles. The surface tension of the molten material may cause the surface material to form small spherical droplets.

The fragmentation of particles could also take place if the particle heating rate was high enough to completely melt the particle before any significant solid crust was formed (alternative path). After initial expansion due to gas evolution, particles exploded instead of ejecting molten material through the surface.

The fragmentation of copper matte particles was more severe for large particles than for small particles. This can be explained in terms of the amount of sulfur initially in the particles, which eventually led to sulfur dioxide buildup. The amounts of gas and heat generated within the large particles as a result of the sulfur oxidation were greater than those produced within the small particles.

The qualitative model described previously provides a reasonable explanation to the observations in this study regarding particle fragmentation. The development of a quantitative model was beyond the scope of this investigation.

IV. CONCLUDING REMARKS

An experimental investigation was conducted to elucidate the main features of the flash-converting furnace shaft. The laboratory tests involved a range of operating conditions and two types of matte particles. Strong interactions among different phenomena occur in this system.

The behaviors of high-grade (72 pct Cu) and low-grade (58 pct Cu) matte particles during oxidation were significantly different. High-grade matte particles tended to oxidize unevenly and fragmented substantially, whereas low-grade matte particles reacted more evenly and experienced no substantial fragmentation. The resistance to particle fragmentation was explained in terms of the iron content in the particle: iron oxide acted as a glue which held the particle together and prevented fragmentation.

The effects of the test variables did not differ significantly for the two matters studied and, in general, had the following order of importance: (1) oxygen-to-matte ratio, (2) particle size of the feed material, and (3) oxygen content in the process gas.

For both mattes, the net effect of increasing the particle size of the feed material was to decrease the fractional conversion, increase the sulfur remaining in the particles, increase the dust generation, and cause a larger decrease in the mean particle size.

The oxygen concentration in the process gas did not significantly affect the system responses when it was varied between 70 and 100 pct in the experiments with both mattes. This was attributed to the changes in the hydrodynamics accompanying the change in oxygen content during the experiments, which might mask the effect of oxygen concentration. Another possible explanation was the blockage of the pores in the oxide layer, by the formation of a dense oxide product, when pure oxygen was used.

The volatilization of the copper species was found to be negligible in both mattes.

In general, small particles in the feed were observed to expand upon oxidation, whereas large particles tended to fragment. The larger amount of sulfur in large particles, leading to sulfur dioxide buildup and particle explosion, was likely the cause for this trend.

The morphology of the reacted particles was observed to change from angular to rounded particles to cenospheres and small droplets during oxidation. The observed transformations agreed well with the general path proposed in the literature for the oxidation of sulfide particles.

The mineralogy of the reacted particles showed that copper and iron oxides were the major oxidation products in the experiments, with minor amounts of elemental copper and Cu-S-O phases.

ACKNOWLEDGMENTS

The authors thank Outokumpu Research Oy for providing one of the mattes and for chemical and particle size analyses of the samples; special thanks are due to Dr. Pekka Taskinen for his technical input and support during this investigation. Acknowledgments are also due to Kennecott Utah Copper Corp. for providing one of the mattes; in particular, thanks are due to Mr. David George for his interest and support for this study. The authors are grateful to their colleague Daniel Swartling for his help during the experimental work. One of the authors (MPT) expresses his gratitude to CONACYT (Consejo Nacional de Ciencia y Tecnologia/National Council of Science and Technology) of Mexico, the Institute of International Education (IIE), the Fulbright Program in the United States, and Universidad de Sonora (Hermosillo, Mexico) for providing the financial support for his graduate program during this work. KSM acknowledges the Academy of Finland and Outokumpu Foundation for providing the financial support for her graduate program.

REFERENCES

1. J.A. Asteljoki, L.K. Bailey, D.B. George, and D.W. Rodolff: *J. Met.*, 1985, vol. 20, pp. 245-50.
2. D.B. George, R.J. Gottling, and C.J. Newman: *Proc. Copper 95-Cobre 95 Int. Conf. IV,* CIM, Montreal, 1995, pp. 41-52.
3. P. Hanniala, I.V. Kojo, and M. Kytö: *Proc. Sulfide Smelting '98: Current and Future Practices*, TMS-AIME, Warrendale, PA, 1998, pp. 239-47.
4. J.A. Asteljoki and S.M.I. Kytö: TMS Technical Paper No. A86-57, TMS-AIME, Warrendale, PA, 1986.
5. H.Y. Sohn and V. Ramachandran: *Proc. Sulfide Smelting '98: Current and Future Practices*, TMS-AIME, Warrendale, PA, 1998, pp. 3-37.
6. R.O. Suominen, A.T. Jokilaakso, P.A. Taskinen, and K.R. Lilius: *Scand. J. Metall.*, 1991, vol. 20, pp. 245-50.
7. R.O. Suominen, A.T. Jokilaakso, P.A. Taskinen, and K.R. Lilius: *Scand. J. Metall.*, 1994, vol. 23, pp. 30-36.
8. Y.H. Kim and N.J. Themelis: *Proc. Reinhardt Schuhmann Int. Symp. on Innovative Technology and Reactor Design in Extractive Metallurgy,* TMS, Warrendale, PA, 1986, pp. 349-69.
9. M. Pérez-Tello, H.Y. Sohn, and J. Löttiger: *Min. Met. Proc.*, 1999, vol. 16, pp. 1-7.
10. G.J. Morgan, A.A. Shook, and J.K. Brimacombe: *Proc. Processing and Handling of Powders and Dusts*, TMS, Warrendale, PA, 1997, pp. 161-78.
11. A. Otero, J.K. Brimacombe, and G.G. Richards: *Proc. Copper 91-Cobre 91,* Pergamon, Elmsford, NY, 1991, pp. 459-73.
12. G.J. Morgan and J.K. Brimacombe: *Metall. Mater. Trans. B,* 1996, vol. 27B, pp. 163-75.
13. A.A. Shook: Ph.D. Thesis, The University of British Columbia, Vancouver BC, Canada, 1992.
14. A.A. Shook, G.G. Richards, and J.K. Brimacombe: *Metall. Mater. Trans. B,* 1995, vol. 26B, pp. 719-30.
15. M. Pérez-Tello: Ph.D. Dissertation, University of Utah, Salt Lake City, UT, 1999.

16. D. Swartling: Master's Thesis, Royal Institute of Technology, Stockholm, 1996.
17. K. Riihilahti, H.Y. Sohn, A. Jokilaakso, and M. Pérez-Tello: *Proc. EPD Congr. 1997*, TMS, Warrendale, PA, 1997, pp. 85-105.
18. K. Riihilahti, H.Y. Sohn, M. Pérez-Tello, and A. Jokilaakso: *Proc. Sulfide Smelting '98: Current and Future Practices*, TMS-AIME, Warrendale, PA, 1998, pp. 261-73.
19. K. Riihilahti: Licenciate Thesis, Helsinki University of Technology, Espoo, Finland, 1997.
20. H.Y. Sohn, M. Pérez-Tello, and K. Riihilahti: *Proc. 3rd. Colloquium on Process Simulation*, Helsinki University of Technology, Espoo, Finland, 1996, pp. 189-217.
21. H.Y. Sohn: *Metall. Trans. B*, 1991, vol. 22B, pp. 737-54.
22. A. Jokilaakso, R. Suominen, P. Taskinen, and K. Lilius: *Trans. Inst. Min. Metall.*, 1991, vol. 100, pp. C79-C90.